AN ANALYTICAL DETERMINATION OF STRESS DISTRIBUTION IN A MOMENT LOADED STIFFENED CYLINDER WITH A CUTOUT

JOHN ALLEN WINFREY, JR.

AN ANALYTICAL DETERMINATION OF STRESS DISTRIBUTION IN A MOMENT LOADED STIFFENED CYLINDER WITH A CUTOUT

A thesis submitted to the faculty of

WEBB INSTITUTE OF NAVAL ARCHITECTURE

in partial satisfaction of the requirements of

the degree of

Master of Science

in

Naval Architecture

by

John Allen Winfrey, Jr.

Lieutenant, USN

June 1959

ABSTRACT

A method for analytically determining the stress distribution in a moment loaded circular semimonocoque cylinder with cutout is presented. The technique employed in the analysis consists of combining the stringers and skin into a smaller number of equivalent stringers and shear membranes and, after determining the bending strain energy of the rings under various shear patterns, deriving the energies of the corresponding idealized structures. Analytical results for the necessary patterns of three idealizations along with the method of application to specific problems are presented in a form suitable for machine computation using Castigliano's Theorem. The comparison of the results of application to an experimental structure with experimental values is also set forth.

TABLE OF CONTENTS

CHAPTER I

INTRODUCTION, STATEMENT OF PROBLEM, AND ORGANIZATION

I. INTRODUCTION

Because of the increasing demand for high performance rocket and missile systems, refined structural design and stress prediction methods have become very important. Most such techniques are, however, complicated and require the services of high grade engineering personnel for their use. On the other hand, the construction of experimental models for test is equally expensive and, if the results lead to redesign, such models are difficult to restructure.

Of particular interest are methods which lead to reasonable stress prediction for structures with cutouts such as are required for instrument and fuel system access ports. Since overall weight is a vital concern, necessary reinforcement of these areas must be efficiently done. If the stress predictions can be made with sufficient accuracy, consistency, and speed, the development time may be significantly reduced.

II. THE PROBLEM

It was the purpose of this study (1) to devise a standard method of analysis for the preliminary prediction of stresses in cylindrical semimonocoque shells with cutout when loaded in pure bending; (2) to present the results in such a manner that they may be used without excessive re-analysis to predict stresses in experimental structures; and (3) to compare the results of the analysis with a set of experimental results.

III. ORGANIZATION

Chapter II will contain a discussion of the previous related studies and the differences between them and this study. Also included will be a definition of the various special terms used.

Chapter III is a discussion of the structural idealization, the general method of analysis , and the steps of the structure analysis.

Chapter IV presents a summary of the results of the analysis and the author's conclusions.

Appendix I illustrates the stepwise analysis of a representative structure.

Appendix II presents the results of a comparison between analytical and experimental results.

CHAPTER II

RELATED STUDIES AND DEFINITIONS OF TERMS

I. RELATED STUDIES

The method of analysis used in this thesis was suggested by a method for handling redundant structures introduced by Professor W. R. Jensen in his Advanced Structures course at Webb Institute of Naval Architecture. Reference (1) outlines its application to a test cylinder. Professor Jensen made his personal notes covering additional work in the area fully available to this author.

A closely related method of analysis is presented in reference (3). Basically it is a perturbation load technique in which individual cancellation loads are placed at the boundaries of the desired cutout in an analytical structure whose external load system corresponds to the physical structure. The stress distribution of the structure without cutout is presumed to be known and reference (4) supplies tables of coefficients to calculate the effect of each type of cancellation load throughout the structure (i.e. the resulting stress distribution in the unloaded structure in the vicinity of the applied unit perturbation loads). In application, then, perturbation

loads in magnitude and orientation necessary to cancel existing stresses in the loaded whole structure are applied to the boundaries of the desired cutout and their associated stress distributions are superimposed on the existing pattern. The resultant stresses represent the distribution in the loaded cylinder with cutout. Reference (5) shows an excellent agreement with the data of reference (2).

In the author's opinion the two foregoing studies are the only ones sufficiently close to the simplified analysis being sought to be pertinent.

II. DEFINITIONS OF SPECIAL TERMS USED

Semimonocoque. As used herein, this term denotes a structure of uniform thickness with regularly spaced stiffeners in the form of ring frames and stringers.

Orthogonal. As used herein, this term designates a property of loads or load systems. When more than one load is applied to a structure simultaneously the effects of each may be considered independently if they are orthogonal. The energy expression for the loaded structure will contain no cross-product terms between the several loads or load systems.

CHAPTER III

IDEALIZATION AND METHOD OF ANALYSIS

I. IDEALIZATION

The types of structures with which this thesis is concerned (i.e. cylindrical semimonocoque) suggest, by their physical appearance, the kind of idealized structure which will be used. It will consist of rings, panels, and stringers which have the following characteristics:

1. The rings are loaded by shear flows only which act to produce ring bending.
2. The panels are loaded by shear flows only. Their thickness is equal to the thickness of panels in the actual structure so that they will have the same effectiveness for carrying the shears as do panels in the actual structure.
3. The stringers take longitudinal loads and longitudinal shear flows and have effective cross sectional areas which include the longitudinal load carrying capacity of the skin of the actual structure.

Three idealizations, differing only in the number of stringers involved, were chosen for analysis. In general,

the number of stringers determines the complexity of the analysis. For this thesis, idealizations with six, eight, and twelve stringers were chosen.

II. METHOD OF ANALYSIS

Having chosen an idealization it was desired to set up the minimum number of independent shear flow and force patterns which, by their subsequent combinations, would produce any possible loading pattern in the idealized structure. It is to be noted that, once a ring shear flow pattern is fixed, the pattern of panel shear flows and stringer forces is also fixed. Figure III - 1 illustrates this principle. The problem, then, reduces to that of determining the number of independent shear flow patterns which may be imposed upon one ring of the idealization. Since shears must remain constant on the ring segments between stringers, must produce no net vertical or horizontal forces, and must produce no net torque about an axis thru the center and perpendicular to the plane of the ring, the number of patterns is limited to the total number of shear segments minus the number of static equilibrium conditions (i.e., in the six stringer ring, 6-3:3 independent patterns).

The applied load, pure bending, requires that the

Figure III - 1

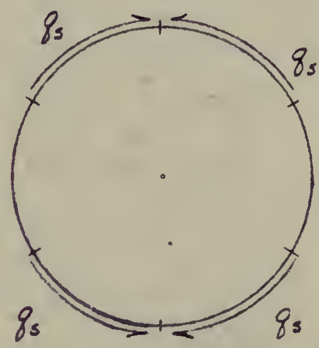

Assumed ring shear flow pattern

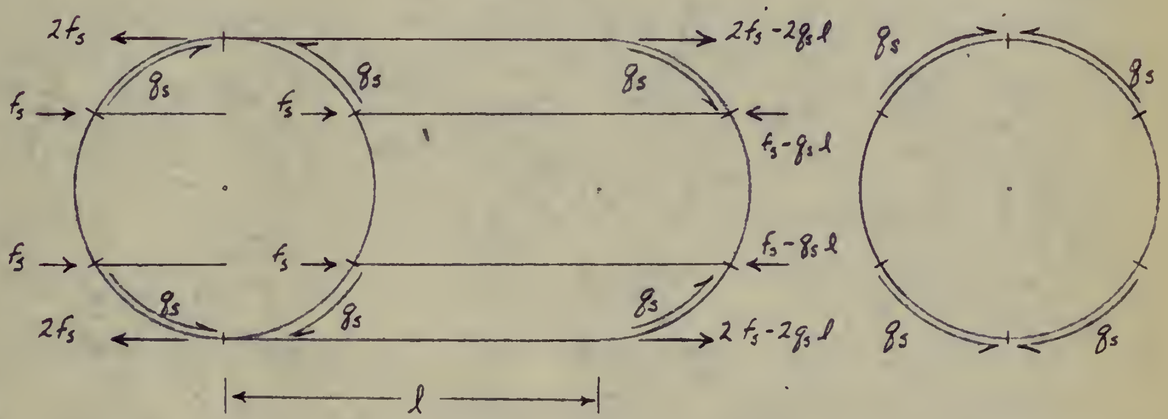

Resulting bay shear flow and stringer force pattern

Note that the top and bottom stringers have twice the load because shear flows act on both sides of these stringers.

line of intersection of its action plane with the ring plane be an axis of symmetry. If this line passes thru segments of the ring rather than thru stringer points the segments may have no shear. In the six stringer case, then, only one pattern of shear flow would be available, figure III-2. For this reason, as well as the fact that some work (Ref. (1)) had already been done with symmetry thru stringers, it was decided to place the plane of action thru stringers. It should be noted that this makes the validity of the comparison with the selected experimental data (Ref. (2)) somewhat doubtful. This point will be covered in Chapter IV and Appendix II.

For convenience it was decided to designate individual ring shear flow patterns by the type of symmetry possessed about the vertical and horizontal axes. With S standing for Symmetry and A standing for Antisymmetry, the first letter of the hyphenated pair in a parenthesis designates the type of symmetry about the vertical axis while the second letter designates the type of symmetry about the horizontal axis.

Before choosing the ring shear patterns, one more consideration was taken into account - orthogonality of load systems. As defined in Chapter II, it is a property of orthogonal load systems that the strain energy of a structure loaded by several such systems is equal to the

Figure III - 2

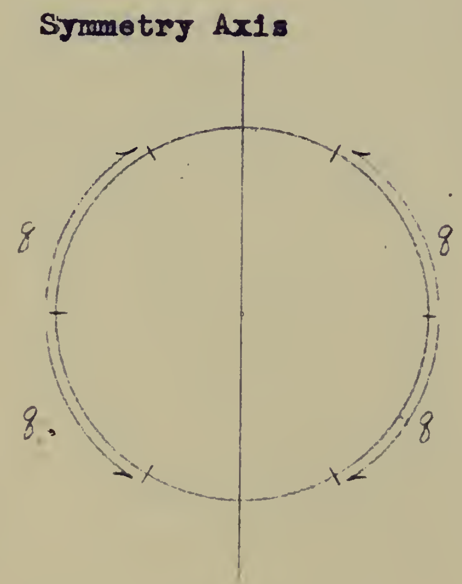

This figure demonstrates that, if a symmetry axis is put thru the panels, the six stringer idealization is limited to one shear pattern, (S-S). No other (S-S) nor (S-A) pattern is possible which satisfies static equilibrium.

sum of the strain energies of the structure loaded by each separately. The coefficients of terms containing load cross products are equal to zero. Patterns with different symmetry are orthogonal, but, if a choice existed among patterns with the same symmetry, the ones chosen were those which were orthogonal.

In summary, then, ring shear patterns must conform to the following conditions:

1. Static equilibrium - necessary condition.
2. Vertical axis of symmetry - necessary condition.
3. Orthogonality - desireable condition.

The actual ring shear patterns chosen were arrived at by trial and error. An interesting by-product of this process was the data for table III-1 which gives the distribution of ring shear patterns by symmetry type for each of the three idealizations. The proof of this table for the six stringer idealization is given in Appendix I, but it was not proven for the eight and twelve stringer cases. Table III-1 is presented primarily as a point of interest.

Once the ring patterns were chosen, corresponding half structures were set up (the structure is symmetrical about its centerline plane). For a given pattern the ring bending strain energy was computed and expressed as one-half the square of the shear flow multiplied by a

Table III - 1

	Ring Shear Patterns			
Ideal.Str.	(S-S)	(S-A)	(A-A)	(A-S)
6 Stringer	1	1	1	0
8 Stringer	2	1	1	1
12 Stringer	3	2	2	2

Distribution of Ring Shear Patterns by Symmetry Type for Idealized Strutures.

"flexibility factor." This factor is the same for any ring loaded with the given pattern. The half-structure was considered on a bay by bay basis as demonstrated in Appendix I, and the loadings on the successive bays starting at the half-bay (the center bay of the overall structure) were determined. The strain energy from stringers, panels, and rings was determined and the sum gave the strain energy of the half-structure.

If loads are orthogonal, the sum of the strain energies for each pattern is equal to the strain energy of the idealized structure loaded by the combined patterns. Orthogonality was checked for patterns of like symmetry.

III. SUMMARY

The steps of the analysis are:

1. Choose an idealization.
2. Select ring shear patterns.
3. For each pattern set up the half-structure.
4. For each pattern calculate the ring "Flexibility Factor."
5. For each pattern, on a bay by bay basis, calculate the energy matrix factors.

Note that the combination of the patterns is not done in the analysis. This step is taken when the results are

applied to a given physical structure since only then will the boundary conditions be known (i.e. the required relationships between the pattern shears and forces and the forces applied to the structure). The complete analysis of a particular idealization consists of the matrices which correspond to the ring shear patterns for the idealization. These are found in Chapter IV for each of the three idealizations.

CHAPTER IV

SUMMARY OF RESULTS AND CONCLUSIONS

I. SUMMARY OF RESULTS

The nature of the results indicates that the best method of presentation is in the form of figures and energy matrices. They are so presented on pages 17 to 32 . It is intended by this form of presentation to make the results available in the most compact and useable form possible. The figures which accompany the results are intended to assist the reader in visualizing the structure to which the matrix applies. The six stringer idealization is presented in its entirety for both symmetry patterns while, for the eight and twelve stringer structures, only a sample bay (the half-bay, bay number (1)) is illustrated for each pattern. Note that stringer force values are diminished as they propogate thru the structure and terminate in a force designated by a capital letter. The end of the structure is considered as built into a rigid wall so that the moment of inertia of the end "ring" is considered to approach infinity (i.e. its flexibility factor is zero). The meaning of the physical constants is summarized in table IV - 1.

The idealizations of this thesis are all for a nine bay structure because the most readily available test data (Ref. (2)) were taken from such a structure. If application is desired to a structure having a different number of bays, the matrices must be altered. The step by step analysis of one pattern of the six stringer idealization is presented in Appendix I so that a model is available for anyone wishing to make such alterations.

TABLE IV - 1

TABLE OF MATRIX SYMBOL DEFINITIONS

q - Shear flow.

R - Radius to the neutral axis of the skin.

ϕR - Radius to the neutral axis of the skin-ring combination.

l - Length of one bay.,

t - Thickness of the skin.

A - Cross-sectional area of the idealized stringer.

E - Elastic Modulus of the structure material.

G - Shear Modulus of the structure material.

I - Moment of Inertia of a cross-section of the skin-ring combination about its neutral axis.

Underlined terms are taken from the physical structure. A is computed as follows:

$$A = \frac{N}{n}(Ast) + \frac{1}{n}\, 2\pi R t,$$

where

N = Number of physical stringers,

n = Number of idealized stringers,

Ast = Cross-sectional area of the physical stringer.

$$) + \varphi^2\left(\frac{5\pi}{4} - \frac{3\sqrt{3}}{2}\right)\Big]$$

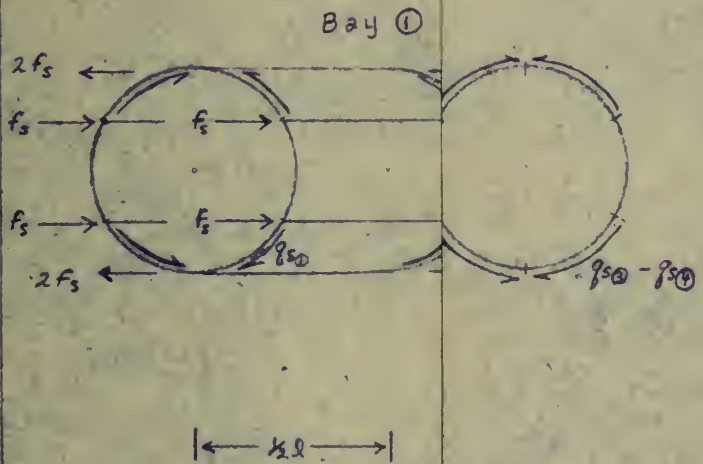

s final ring is
lt into rigid
ructure (I → ∞).

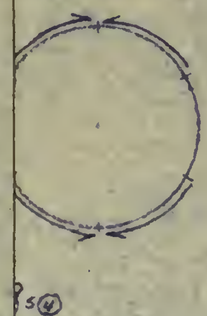

SIX STRINGER (S - S)
IDEALIZED
SEMI-STRUCTURE

$$U_{R6(S-S)} = \frac{1}{2}\beta_1 q_s^2$$

$$\beta_1 = \frac{\Phi R^5}{EI}\left[\frac{2\pi^3}{81} + \varphi\left(\frac{8\pi}{3} - 6\sqrt{3}\right) + \varphi^2\left(\frac{5\pi}{4} - \frac{3\sqrt{3}}{2}\right)\right]$$

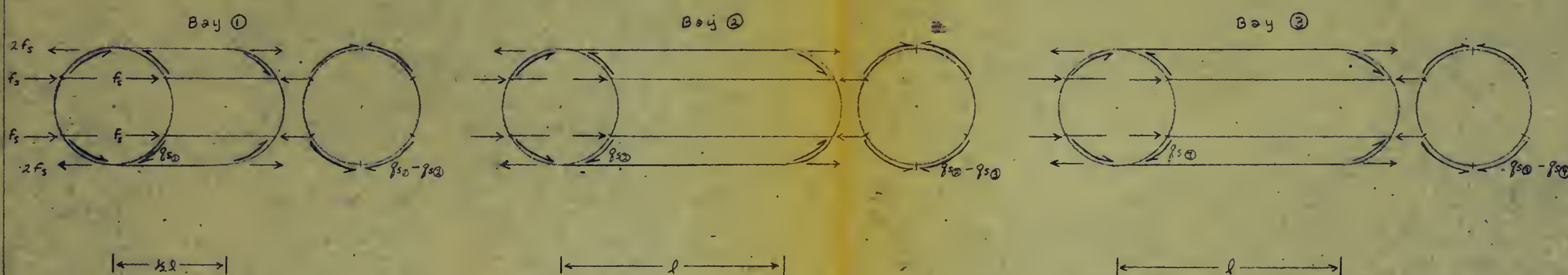

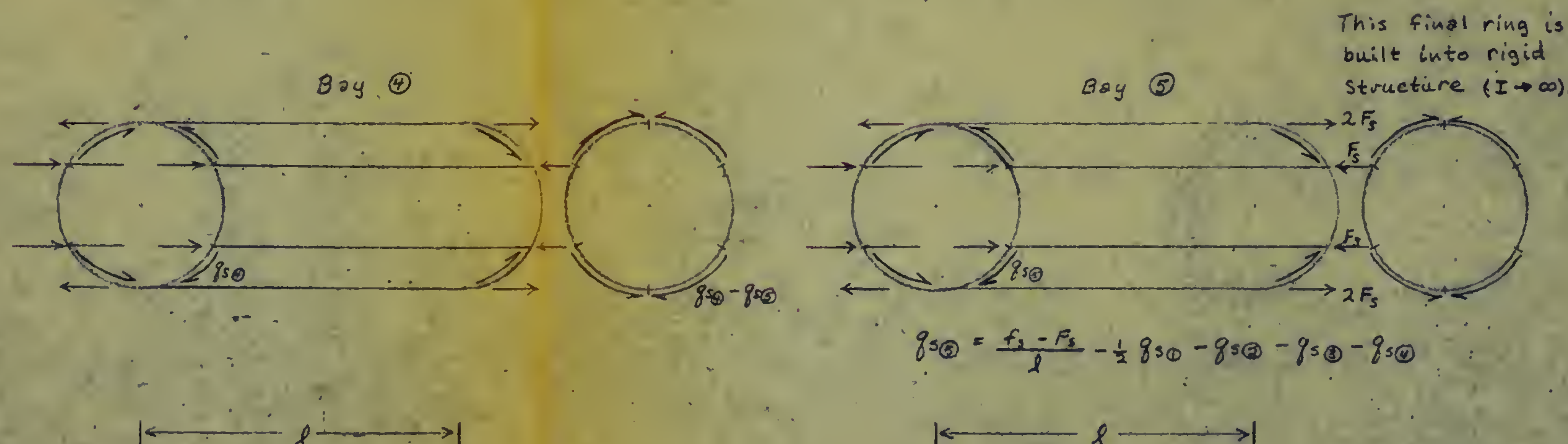

$$q_{s⑤} = \frac{f_s - F_s}{l} - \frac{1}{2}q_{s①} - q_{s②} - q_{s③} - q_{s④}$$

SIX STRINGER (S - S)
IDEALIZED
SEMI-STRUCTURE

$$U_{R6(S-A)} = \tfrac{1}{2}\,\beta_2\, q_a^2$$

$$\beta_2 = \frac{\varphi R^5}{EI}\left[\frac{\pi^3}{54} + \varphi(4\pi - 8\sqrt{3}) + \varphi^2\left(\frac{4\pi}{3} - 2\sqrt{3}\right)\right]$$

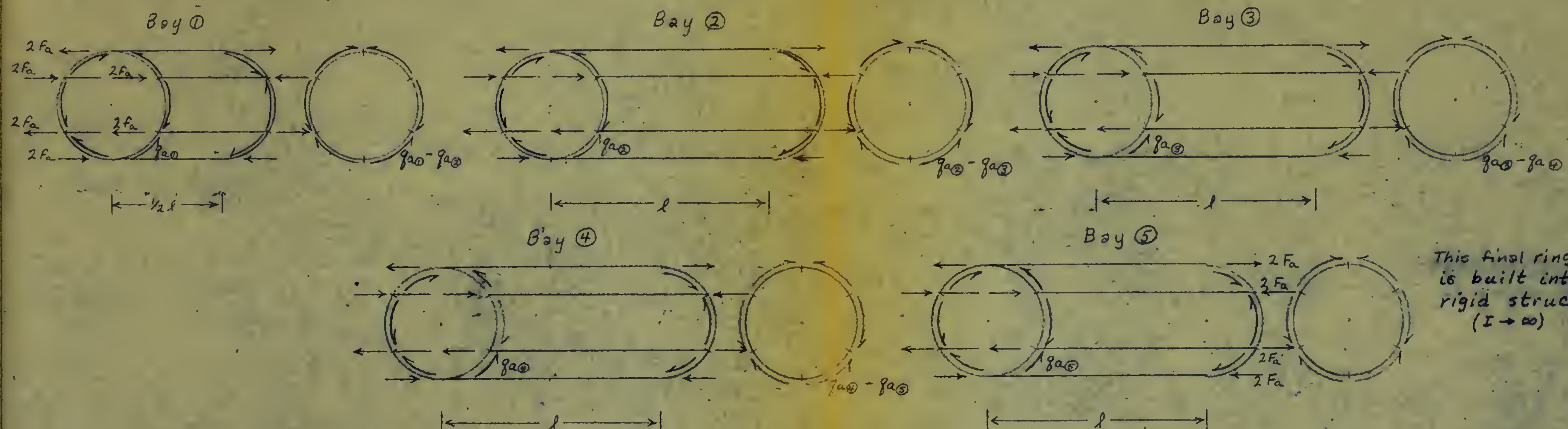

$$q_{a5} = \frac{F_a - F_a}{l} - \tfrac{1}{2}q_{a1} - q_{a2} - q_{a3} - q_{a4}$$

This final ring is built into rigid structure ($I \rightarrow \infty$)

SIX STRINGER (S-A)
IDEALIZED
SEMI-STRUCTURE

In equation form, the (S-S) pattern strain energy is

$$
\begin{aligned}
2U_{s6}(s-s) = {} & \left(\frac{4\pi R}{3\ell tG}+\frac{46\ell}{AE}+\frac{\beta_1}{\ell^2}\right)(f_s^{\,2}) + 2\left(\frac{-4\pi R}{3\ell tG}+\frac{2\ell}{AE}-\frac{\beta_1}{\ell^2}\right)(f_s)(F_s) + 2\left(\frac{-2\pi R}{3\ell tG}-\frac{43\ell}{2AE}-\frac{\beta_1}{2\ell^2}\right)(f_s)(q_{s\textcircled{1}}\ell) \\
& + 2\left(\frac{-4\pi R}{3\ell tG}-\frac{34\ell}{AE}-\frac{\beta_1}{\ell^2}\right)(f_s)(q_{s\textcircled{2}}\ell) + 2\left(\frac{-4\pi R}{3\ell tG}-\frac{22\ell}{AE}-\frac{\beta_1}{\ell^2}\right)(f_s)(q_{s\textcircled{3}}\ell) + 2\left(\frac{-4\pi R}{3\ell tG}-\frac{10\ell}{AE}-\frac{2\beta_1}{\ell^2}\right)(f_s)(q_{s\textcircled{4}}\ell) \\
& + \left(\frac{4\pi R}{3\ell tG}+\frac{4\ell}{AE}+\frac{\beta_1}{\ell^2}\right)(F_s^{\,2}) + 2\left(\frac{2\pi R}{3\ell tG}-\frac{\ell}{AE}+\frac{\beta_1}{2\ell^2}\right)(F_s)(q_{s\textcircled{1}}\ell) + 2\left(\frac{4\pi R}{3\ell tG}-\frac{2\ell}{AE}+\frac{\beta_1}{\ell^2}\right)(F_s)(q_{s\textcircled{2}}\ell) \\
& + 2\left(\frac{4\pi R}{3\ell tG}-\frac{2\ell}{AE}+\frac{\beta_1}{\ell^2}\right)(F_s)(q_{s\textcircled{3}}\ell) + 2\left(\frac{4\pi R}{3\ell tG}-\frac{2\ell}{AE}+\frac{2\beta_1}{\ell^2}\right)(F_s)(q_{s\textcircled{4}}\ell) + \left(\frac{3\pi R}{3\ell tG}+\frac{21\ell}{2AE}+\frac{5\beta_1}{4\ell^2}\right)(q_{s\textcircled{1}}\ell)^2 \\
& + 2\left(\frac{2\pi R}{3\ell tG}+\frac{17\ell}{AE}-\frac{\beta_1}{2\ell^2}\right)(q_{s\textcircled{1}}\ell)(q_{s\textcircled{2}}\ell) + 2\left(\frac{2\pi R}{3\ell tG}+\frac{11\ell}{AE}+\frac{\beta_1}{2\ell^2}\right)(q_{s\textcircled{1}}\ell)(q_{s\textcircled{3}}\ell) + 2\left(\frac{2\pi R}{3\ell tG}+\frac{5\ell}{AE}+\frac{\beta_1}{\ell^2}\right)(q_{s\textcircled{1}}\ell)(q_{s\textcircled{4}}\ell) \\
& + \left(\frac{8\pi R}{3\ell tG}+\frac{32\ell}{AE}+\frac{3\beta_1}{\ell^2}\right)(q_{s\textcircled{2}}\ell)^2 + 2\left(\frac{4\pi R}{3\ell tG}+\frac{22\ell}{AE}\right)(q_{s\textcircled{2}}\ell)(q_{s\textcircled{3}}\ell) + 2\left(\frac{4\pi R}{3\ell tG}+\frac{10\ell}{AE}+\frac{2\beta_1}{\ell^2}\right)(q_{s\textcircled{2}}\ell)(q_{s\textcircled{4}}\ell) \\
& + \left(\frac{8\pi R}{3\ell tG}+\frac{20\ell}{AE}+\frac{3\beta_1}{\ell^2}\right)(q_{s\textcircled{3}}\ell)^2 + 2\left(\frac{4\pi R}{3\ell tG}+\frac{10\ell}{AE}+\frac{\beta_1}{\ell^2}\right)(q_{s\textcircled{3}}\ell)(q_{s\textcircled{4}}\ell) + \left(\frac{8\pi R}{3\ell tG}-\frac{8\ell}{AE}+\frac{5\beta_1}{\ell^2}\right)(q_{s\textcircled{4}}\ell)^2.
\end{aligned}
$$

Each of the terms in the above energy expression contains a coefficient times a second degree load product. Such an arrangement suggests the use of the less "cluttered" matrix form and, since modern digital computers are often adjusted to solve matrix inputs, this form was adopted. Conversion is accomplished by laying out load rows and columns as on page (19C) and placing each coefficient in the block corresponding to the intersection of the column of one load with the row of the other. Since a matrix is symmetric about its major diagonal (i.e. load squared terms), non-squared load product positions occur in pairs

and one-half of the coefficient is placed in each. For the same reason, only one half of the matrix need be filled in since corresponding blocks in the other half are identical. Additional information on general matrix use may be found in reference (6) while its specific application to structural analysis is well illustrated in reference (7).

$U_{66(S-S)} = \frac{1}{2}$

	f_s	F_s	$q_{s\textcircled{1}}\ell$	$q_{s\textcircled{2}}\ell$	$q_{s\textcircled{3}}\ell$	$q_{s\textcircled{4}}\ell$
f_s	$\frac{4\pi R}{3\ell tG} + \frac{46\ell}{AE} + \frac{\beta_1}{\ell^2}$	$-\frac{4\pi R}{3\ell tG} + \frac{2\ell}{AE} - \frac{\beta_1}{\ell^2}$	$-\frac{2\pi R}{3\ell tG} - \frac{43\ell}{2AE} - \frac{\beta_1}{2\ell^2}$	$-\frac{4\pi R}{3\ell tG} - \frac{34\ell}{AE} - \frac{\beta_1}{\ell^2}$	$-\frac{4\pi R}{3\ell tG} - \frac{22\ell}{AE} - \frac{\beta_1}{\ell^2}$	$-\frac{4\pi R}{3\ell tG} - \frac{10\ell}{AE} - \frac{2\beta_1}{\ell^2}$
F_s		$\frac{4\pi R}{3\ell tG} + \frac{4\ell}{AE} + \frac{\beta_1}{\ell^2}$	$\frac{2\pi R}{3\ell tG} - \frac{\ell}{AE} + \frac{\beta_1}{2\ell^2}$	$\frac{4\pi R}{3\ell tG} - \frac{2\ell}{AE} + \frac{\beta_1}{\ell^2}$	$\frac{4\pi R}{3\ell tG} - \frac{2\ell}{AE} + \frac{\beta_1}{\ell^2}$	$\frac{4\pi R}{3\ell tG} - \frac{2\ell}{AE} + \frac{2\beta_1}{\ell^2}$
$q_{s\textcircled{1}}\ell$			$\frac{3\pi R}{3\ell tG} + \frac{21\ell}{2AE} + \frac{5\beta_1}{4\ell^2}$	$\frac{2\pi R}{3\ell tG} + \frac{17\ell}{AE} - \frac{\beta_1}{2\ell^2}$	$\frac{2\pi R}{3\ell tG} + \frac{11\ell}{AE} + \frac{\beta_1}{2\ell^2}$	$\frac{2\pi R}{3\ell tG} + \frac{5\ell}{AE} + \frac{\beta_1}{\ell^2}$
$q_{s\textcircled{2}}\ell$				$\frac{8\pi R}{3\ell tG} + \frac{32\ell}{AE} + \frac{3\beta_1}{\ell^2}$	$\frac{4\pi R}{3\ell tG} + \frac{22\ell}{AE}$	$\frac{4\pi R}{3\ell tG} + \frac{10\ell}{AE} + \frac{2\beta_1}{\ell^2}$
$q_{s\textcircled{3}}\ell$					$\frac{8\pi R}{3\ell tG} + \frac{20\ell}{AE} + \frac{3\beta_1}{\ell^2}$	$\frac{4\pi R}{3\ell tG} + \frac{10\ell}{AE} + \frac{\beta_1}{\ell^2}$
$q_{s\textcircled{4}}\ell$						$\frac{8\pi R}{3\ell tG} + \frac{8\ell}{AE} + \frac{5\beta_1}{\ell^2}$

SIX STRINGER

(S-S) PATTERN

ENERGY MATRIX

$U_{S6(S-A)} = \frac{1}{2}$

	f_a	F_a	$q_{a①} l$	$q_{a②} l$	$q_{a③} l$	$q_{a④} l$
f_a	$\frac{2\pi R}{ltG} + \frac{92 l}{AE} + \frac{\beta_2}{l^2}$	$-\frac{2\pi R}{ltG} + \frac{4l}{AE} - \frac{\beta_2}{l^2}$	$-\frac{\pi R}{ltG} - \frac{43 l}{AE} - \frac{\beta_2}{2l^2}$	$-\frac{2\pi R}{ltG} - \frac{68 l}{AE} - \frac{\beta_2}{l^2}$	$-\frac{2\pi R}{ltG} - \frac{44 l}{AE} - \frac{\beta_2}{l^2}$	$-\frac{2\pi R}{ltG} - \frac{20 l}{AE} - \frac{2\beta_2}{l^2}$
F_a		$\frac{2\pi R}{ltG} + - \frac{8l}{AE} + \frac{\beta_2}{l^2}$	$\frac{\pi R}{ltG} - \frac{2l}{AE} + \frac{\beta_2}{2l^2}$	$\frac{2\pi R}{ltG} - \frac{4l}{AE} + \frac{\beta_2}{l^2}$	$\frac{2\pi R}{ltG} - \frac{4l}{AE} + \frac{\beta_2}{l^2}$	$\frac{2\pi R}{ltG} - \frac{4l}{AE} + \frac{2\beta_2}{l^2}$
$q_{a①} l$			$\frac{3\pi R}{2ltG} + \frac{21 l}{AE} + \frac{5\beta_2}{4l^2}$	$\frac{\pi R}{ltG} + \frac{34 l}{AE} - \frac{\beta_2}{2l^2}$	$\frac{\pi R}{ltG} + \frac{22 l}{AE} + \frac{\beta_2}{2l^2}$	$\frac{\pi R}{ltG} + \frac{10 l}{AE} + \frac{\beta_2}{l^2}$
$q_{a②} l$				$\frac{4\pi R}{ltG} + \frac{64 l}{AE} + \frac{3\beta_2}{l^2}$	$\frac{2\pi R}{ltG} + \frac{44 l}{AE}$	$\frac{2\pi R}{ltG} + \frac{20 l}{AE} + \frac{2\beta_2}{l^2}$
$q_{a③} l$					$\frac{4\pi R}{ltG} + \frac{40 l}{AE} + \frac{3\beta_2}{l^2}$	$\frac{2\pi R}{ltG} + \frac{20 l}{AE} + \frac{\beta_2}{l^2}$
$q_{a④} l$						$\frac{4\pi R}{ltG} + \frac{16 l}{AE} + \frac{5\beta_2}{l^2}$

SIX STRINGER

(S-A) PATTERN

ENERGY MATRIX

$$U_{R8(s-s)_1} = \frac{1}{2}\beta_1 q_{s1}^2 \qquad \beta_1 = \frac{R^5}{EI}\left[\phi^3(2\pi-4)+\phi^2(4\pi-16)+\phi\left(\frac{\pi}{24}^{3}\right)\right]$$

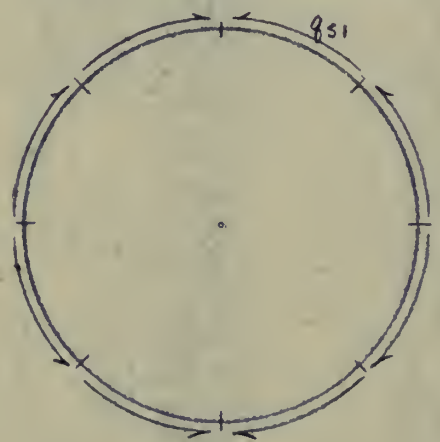

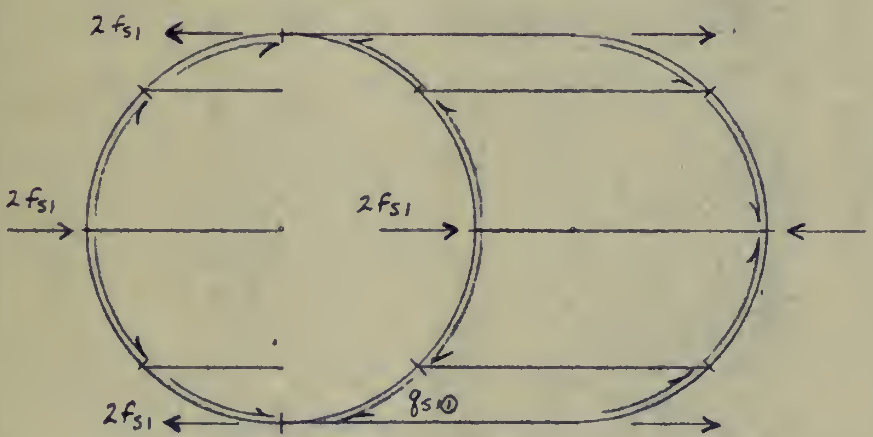

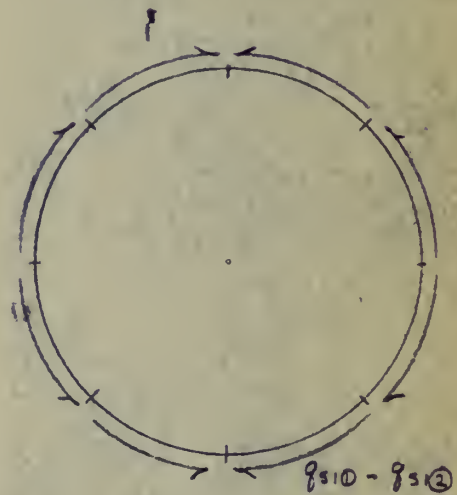

EIGHT STRINGER IDEALIZATION

(S-S)$_1$ PATTERN

Ring Energy and Sample Bay

$$U_{R8(S-S)_2} = \frac{1}{2}\beta_2\, q_{S2}^2 \qquad \beta_2 = \frac{R^5}{EI}\left[\varphi^3\left\{2\pi(2-\sqrt{2}) + 8(1-\sqrt{2})\right\} + \varphi^2\left\{4\pi + 32(1-\sqrt{2})\right\} + \varphi\left(\frac{\pi^3}{96}\right)\right]$$

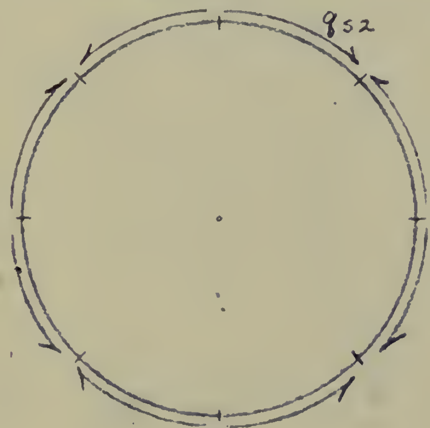

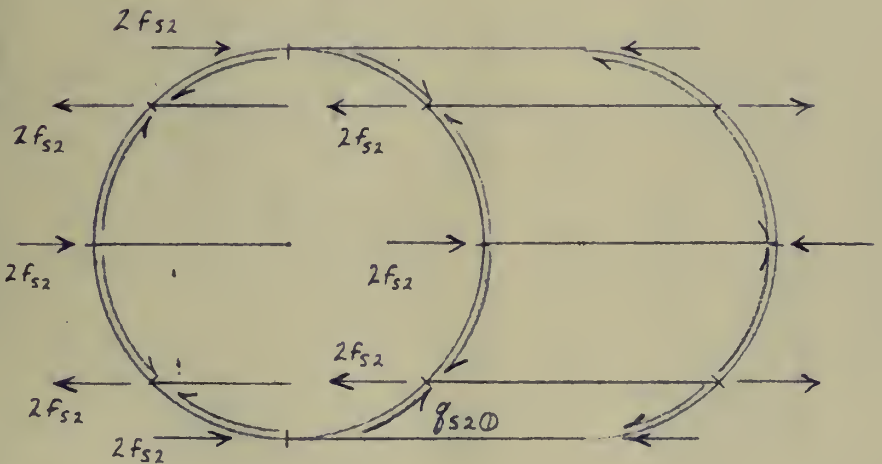

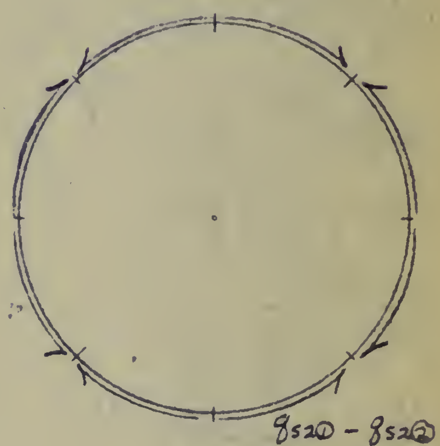

EIGHT STRINGER IDEALIZATION

$(S\text{-}S)_2$ PATTERN

Ring Energy and Sample Bay

$$U_{R8(S-A)} = \frac{1}{2}\,\beta_3\, q_a^2 \qquad \beta_3 = \frac{R^5}{EI}\left[\varphi^3\left(\frac{3\pi}{4} - 2\right) + \varphi^2\left\{4\pi\left(2-\sqrt{2}\right) - 8\right\} + \varphi\left\{\frac{\pi^3}{3}\left(1 - \frac{11\sqrt{2}}{16}\right)\right\}\right]$$

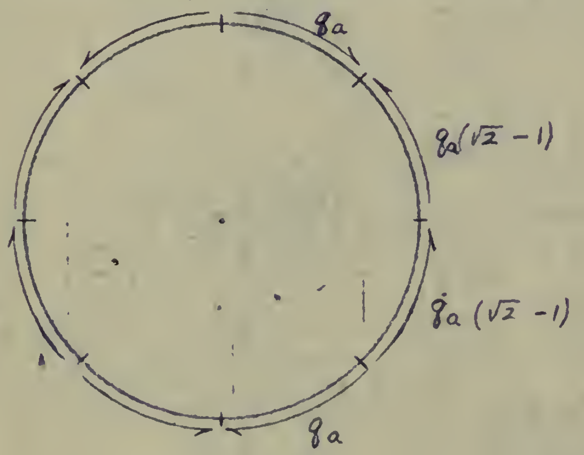

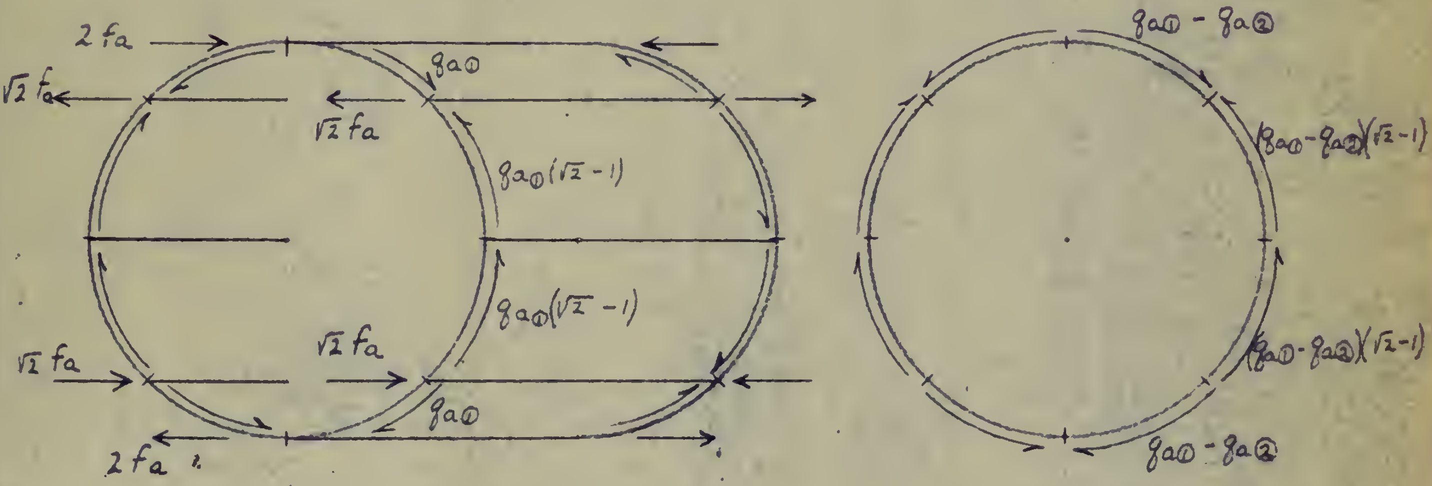

EIGHT STRINGER IDEALIZATION

(S-A) PATTERN

Ring Energy and Sample Bay

$$\bar{U}_{s8(S-S)_1} = \frac{1}{2}$$

	f_{s_1}	F_{s_1}	$g_{s_1①}\ell$	$g_{s_1②}\ell$	$g_{s_1③}\ell$	$g_{s_1④}\ell$
f_{s_1}	$\frac{2\pi R}{\ell tG} + \frac{184\ell}{3AE} + \frac{\beta_1}{\ell^2}$	$-\frac{2\pi R}{\ell tG} + \frac{8\ell}{3AE} - \frac{\beta_1}{\ell^2}$	$-\frac{\pi R}{\ell tG} - \frac{86\ell}{3AE} - \frac{\frac{1}{2}\beta_1}{\ell^2}$	$-\frac{2\pi R}{\ell tG} - \frac{136\ell}{3AE} - \frac{\beta_1}{\ell^2}$	$-\frac{2\pi R}{\ell tG} - \frac{88\ell}{3AE} - \frac{\beta_1}{\ell^2}$	$-\frac{2\pi R}{\ell tG} - \frac{40\ell}{3AE} - \frac{2\beta_1}{\ell^2}$
F_{s_1}		$\frac{2\pi R}{\ell tG} + \frac{16\ell}{3AE} + \frac{\beta_1}{\ell^2}$	$\frac{\pi R}{\ell tG} - \frac{4\ell}{3AE} + \frac{\frac{1}{2}\beta_1}{\ell^2}$	$\frac{2\pi R}{\ell tG} - \frac{8\ell}{3AE} + \frac{\beta_1}{\ell^2}$	$\frac{2\pi R}{\ell tG} - \frac{8\ell}{3AE} + \frac{\beta_1}{\ell^2}$	$\frac{2\pi R}{\ell tG} - \frac{8\ell}{3AE} + \frac{2\beta_1}{\ell^2}$
$g_{s_1①}\ell$			$\frac{\frac{3}{2}\pi R}{\ell tG} + \frac{42\ell}{3AE} + \frac{\frac{5}{4}\beta_1}{\ell^2}$	$\frac{\pi R}{\ell tG} + \frac{68\ell}{3AE} - \frac{\frac{1}{2}\beta_1}{\ell^2}$	$\frac{\pi R}{\ell tG} + \frac{44\ell}{3AE} + \frac{\frac{1}{2}\beta_1}{\ell^2}$	$\frac{\pi R}{\ell tG} + \frac{20\ell}{3AE} + \frac{\beta_1}{\ell^2}$
$g_{s_1②}\ell$				$\frac{4\pi R}{\ell tG} + \frac{128\ell}{3AE} + \frac{3\beta_1}{\ell^2}$	$\frac{2\pi R}{\ell tG} + \frac{88\ell}{3AE}$	$\frac{2\pi R}{\ell tG} + \frac{40\ell}{3AE} + \frac{2\beta_1}{\ell^2}$
$g_{s_1③}\ell$					$\frac{4\pi R}{\ell tG} + \frac{80\ell}{3AE} + \frac{3\beta_1}{\ell^2}$	$\frac{2\pi R}{\ell tG} + \frac{40\ell}{3AE} + \frac{\beta_1}{\ell^2}$
$g_{s_1④}\ell$						$\frac{4\pi R}{\ell tG} + \frac{32\ell}{3AE} + \frac{5\beta_1}{\ell^2}$

EIGHT STRINGER

$(S-S)_1$ PATTERN

ENERGY MATRIX

	f_{s2}	F_{s2}	$q_{s2(1)}\ell$	$q_{s2(2)}\ell$	$q_{s2(3)}\ell$	$q_{s2(4)}\ell$
f_{s2}	$\frac{2\pi R}{\ell tG} + \frac{368\ell}{3AE} + \frac{\beta_2}{\ell^2}$	$-\frac{2\pi R}{\ell tG} + \frac{16\ell}{3AE} - \frac{\beta_2}{\ell^2}$	$-\frac{\pi R}{\ell tG} - \frac{172\ell}{3AE} - \frac{\frac{1}{2}\beta_2}{\ell^2}$	$-\frac{2\pi R}{\ell tG} - \frac{272\ell}{3AE} - \frac{\beta_2}{\ell^2}$	$-\frac{2\pi R}{\ell tG} - \frac{176\ell}{3AE} - \frac{\beta_2}{\ell^2}$	$-\frac{2\pi R}{\ell tG} - \frac{80\ell}{3AE} - \frac{2\beta_2}{\ell^2}$
F_{s2}		$\frac{2\pi R}{\ell tG} + \frac{32\ell}{3AE} + \frac{\beta_2}{\ell^2}$	$\frac{\pi R}{\ell tG} - \frac{8\ell}{3AE} + \frac{\frac{1}{2}\beta_2}{\ell^2}$	$\frac{2\pi R}{\ell tG} - \frac{16\ell}{3AE} + \frac{\beta_2}{\ell^2}$	$\frac{2\pi R}{\ell tG} - \frac{16\ell}{3AE} + \frac{\beta_2}{\ell^2}$	$\frac{2\pi R}{\ell tG} - \frac{16\ell}{3AE} + \frac{2\beta_2}{\ell^2}$
$q_{s2(1)}\ell$			$\frac{\frac{3}{2}\pi R}{\ell tG} + \frac{84\ell}{3AE} + \frac{\frac{5}{4}\beta_2}{\ell^2}$	$\frac{\pi R}{\ell tG} + \frac{136\ell}{3AE} - \frac{\frac{1}{2}\beta_2}{\ell^2}$	$\frac{\pi R}{\ell tG} + \frac{88\ell}{3AE} + \frac{\frac{1}{2}\beta_2}{\ell^2}$	$\frac{\pi R}{\ell tG} + \frac{40\ell}{3AE} + \frac{\beta_2}{\ell^2}$
$q_{s2(2)}\ell$				$\frac{4\pi R}{\ell tG} + \frac{256\ell}{3AE} + \frac{3\beta_2}{\ell^2}$	$\frac{2\pi R}{\ell tG} + \frac{176\ell}{3AE}$	$\frac{2\pi R}{\ell tG} + \frac{80\ell}{3AE} + \frac{2\beta_2}{\ell^2}$
$q_{s2(3)}\ell$					$\frac{4\pi R}{\ell tG} + \frac{160\ell}{3AE} + \frac{3\beta_2}{\ell^2}$	$\frac{2\pi R}{\ell tG} + \frac{80\ell}{3AE} + \frac{\beta_2}{\ell^2}$
$q_{s2(4)}\ell$						$\frac{4\pi R}{\ell tG} + \frac{64\ell}{3AE} + \frac{5\beta_2}{\ell^2}$

$$U_{s8\,(S-S)_2} = \frac{1}{2}$$

EIGHT STRINGER

$(S-S)_2$ PATTERN

ENERGY MATRIX

EIGHT STRINGER

(S-A) PATTERN

ENERGY MATRIX

$$k = 4 - 2\sqrt{2}$$

$$U_{s8}(S-A) = \frac{1}{2}$$

	f_a	F_a	$g_{a1\textcircled{1}}\ell$	$g_{a1\textcircled{2}}\ell$	$g_{a1\textcircled{3}}\ell$	$g_{a1\textcircled{4}}\ell$
f_a	$\frac{k\pi R}{\ell t G} + \frac{184\ell}{3AE} + \frac{\beta_3}{\ell^2}$	$-\frac{k\pi R}{\ell t G} + \frac{8\ell}{3AE} - \frac{\beta_3}{\ell^2}$	$-\frac{\frac{1}{2}k\pi R}{\ell t G} - \frac{86\ell}{3AE} - \frac{\frac{1}{2}\beta_3}{\ell^2}$	$-\frac{k\pi R}{\ell t G} - \frac{136\ell}{3AE} - \frac{\beta_3}{\ell^2}$	$-\frac{k\pi R}{\ell t G} - \frac{88\ell}{3AE} - \frac{\beta_3}{\ell^2}$	$-\frac{k\pi R}{\ell t G} - \frac{40\ell}{3AE} - \frac{2\beta_3}{\ell^2}$
F_a		$\frac{k\pi R}{\ell t G} + \frac{16\ell}{3AE} + \frac{\beta_3}{\ell^2}$	$\frac{\frac{1}{2}k\pi R}{\ell t G} - \frac{4\ell}{3AE} + \frac{\frac{1}{2}\beta_3}{\ell^2}$	$\frac{k\pi R}{\ell t G} - \frac{8\ell}{3AE} + \frac{\beta_3}{\ell^2}$	$\frac{k\pi R}{\ell t G} - \frac{8\ell}{3AE} + \frac{\beta_3}{\ell^2}$	$\frac{k\pi R}{\ell t G} - \frac{8\ell}{3AE} + \frac{2\beta_3}{\ell^2}$
$g_{a1\textcircled{1}}\ell$			$\frac{\frac{3}{4}k\pi R}{\ell t G} + \frac{42\ell}{3AE} + \frac{\frac{5}{4}\beta_3}{\ell^2}$	$\frac{\frac{1}{2}k\pi R}{\ell t G} + \frac{68\ell}{3AE} - \frac{\frac{1}{2}\beta_3}{\ell^2}$	$\frac{\frac{1}{2}k\pi R}{\ell t G} + \frac{44\ell}{3AE} + \frac{\frac{1}{2}\beta_3}{\ell^2}$	$\frac{\frac{1}{2}k\pi R}{\ell t G} + \frac{20\ell}{3AE} + \frac{\beta_3}{\ell^2}$
$g_{a1\textcircled{2}}\ell$				$\frac{2k\pi R}{\ell t G} + \frac{128\ell}{3AE} + \frac{3\beta_3}{\ell^2}$	$\frac{k\pi R}{\ell t G} + \frac{88\ell}{3AE}$	$\frac{k\pi R}{\ell t G} + \frac{40\ell}{3AE} + \frac{2\beta_3}{\ell^2}$
$g_{a1\textcircled{3}}\ell$					$\frac{2k\pi R}{\ell t G} + \frac{80\ell}{3AE} + \frac{3\beta_3}{\ell^2}$	$\frac{k\pi R}{\ell t G} + \frac{40\ell}{3AE} + \frac{\beta_3}{\ell^2}$
$g_{a1\textcircled{4}}\ell$						$\frac{2k\pi R}{\ell t G} + \frac{32\ell}{3AE} + \frac{5\beta_3}{\ell^2}$

$$\alpha_1 = \frac{\Phi R^5}{EI}\left[\frac{\pi^3}{24} + \phi(4\pi - 16) + \phi^2(2\pi - 4)\right]$$

$$\alpha_2 = \frac{\Phi R^5}{EI}\left[\frac{7\pi^3}{648} + \phi\left(4\sqrt{3} - 12 + \frac{4\pi}{3}\right) + \phi^2\left(\sqrt{3} - 3 - \frac{\sqrt{3}\pi}{3} + \frac{7\pi}{6}\right)\right]$$

$$\alpha_3 = \frac{\Phi R^5}{EI}\left[\frac{13\pi^3}{324} + \phi\left(16 - 16\sqrt{3} + \frac{8\pi}{3}\right) + \phi^2\left(4 - 4\sqrt{3} + \frac{4\sqrt{3}\pi}{3} - \frac{2\pi}{3}\right)\right]$$

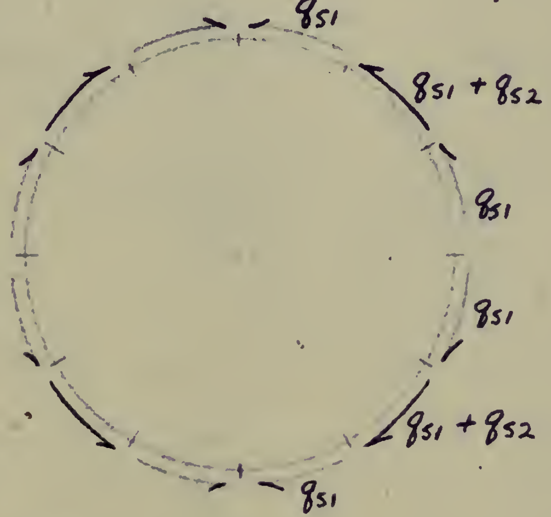

$$U_{R12(S-S)m} = \tfrac{1}{2}\alpha_1 q_{s1}^2 + \tfrac{1}{2}\alpha_2 q_{s2}^2 + \tfrac{1}{2}\alpha_3 q_{s1} q_{s2}$$

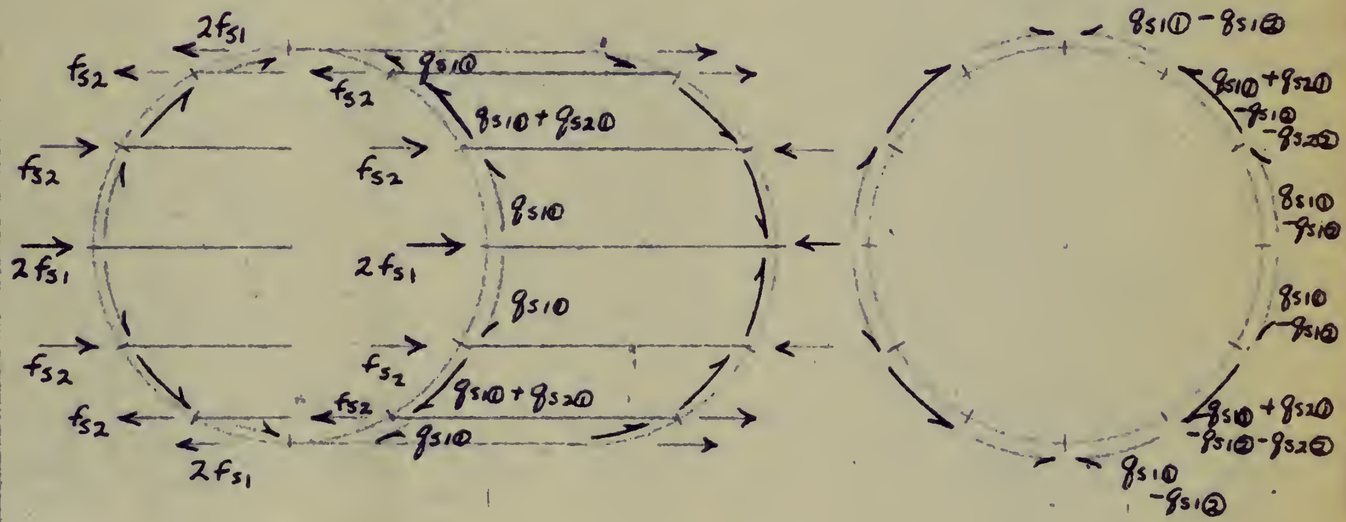

TWELVE STRINGER IDEALIZATION

(S-S)mixed PATTERN

Ring Energy and Sample Bay

$$\beta = \frac{\Phi R^5}{EI}\left[\frac{\pi^3}{162} + \Phi\left(12 - 12\sqrt{3} + \frac{8\pi}{3}\right) + \Phi^2\left(3 - 3\sqrt{3} + \frac{5\pi}{2} - \sqrt{3}\pi\right)\right].$$

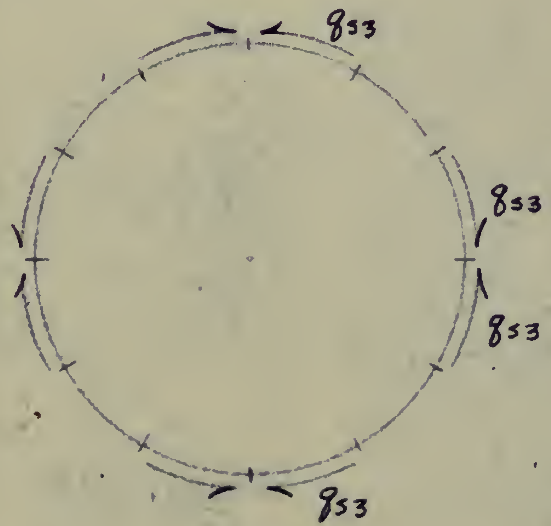

$$U_{R12(S-S)} = \tfrac{1}{2}\,\beta\, q_{s3}^{2}$$

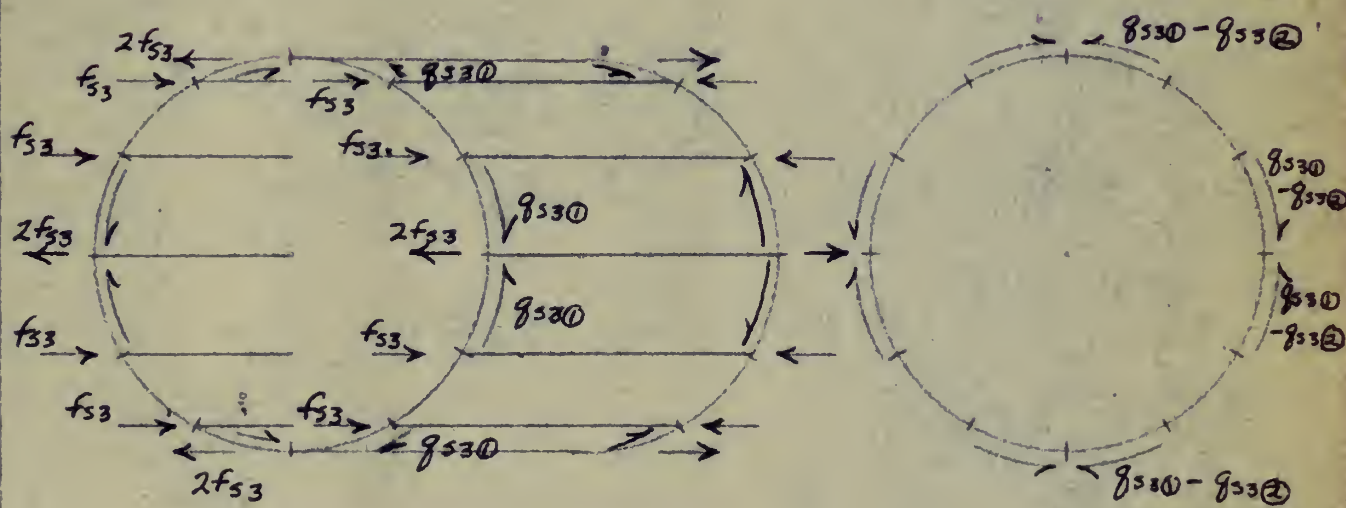

TWELVE STRINGER IDEALIZATION

(S-S) PATTERN

Ring Energy and Sample Bay

$$\gamma_1 = \frac{\Phi R^5}{EI}\left[\frac{\pi^3}{54} + \Phi(4\pi - 8\sqrt{3}) + \Phi^2\left(\frac{4\pi}{3} - 2\sqrt{3}\right)\right]$$

$$\gamma_2 = \frac{\Phi R^5}{EI}\left[\pi^3\left(\frac{11}{162} - \frac{7\sqrt{3}}{216}\right) + \Phi\left(\frac{8\pi}{3} - 4 - 3\sqrt{3}\right) + \Phi^2\left(\frac{71\pi}{144} + \frac{2\sqrt{3}\pi}{9} - \frac{3\sqrt{3}}{4} - 1\right)\right]$$

$$\gamma_3 = \frac{\Phi R^5}{EI}\left[\pi^3\left(\frac{\sqrt{3}}{162} - \frac{1}{108}\right) + \Phi\left(\frac{7\pi^2}{216} + \frac{5\sqrt{3}\pi^2}{54} + 4\pi + \frac{4\sqrt{3}\pi}{3} - 8 - 8\sqrt{3}\right) + \Phi^2\left(\frac{37\pi}{36} + \frac{29\sqrt{3}\pi}{216} - \frac{7}{48} - \frac{155\sqrt{3}}{72}\right)\right]$$

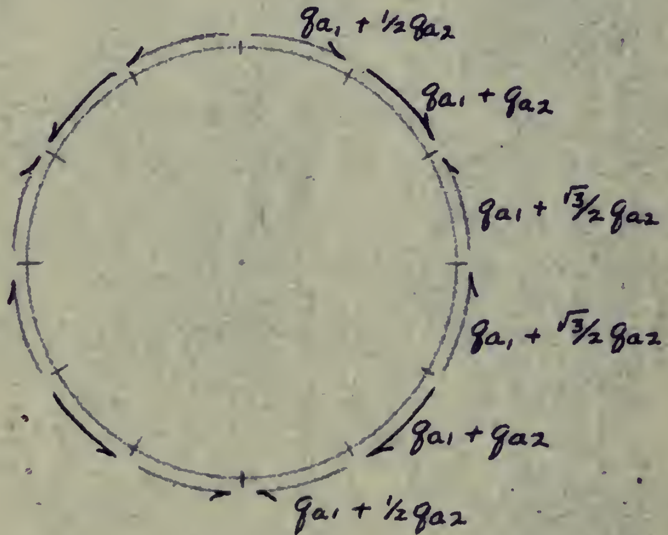

$$U_{R12(S-A)_m} = \tfrac{1}{2}\gamma_1 q_{a1}^2 + \tfrac{1}{2}\gamma_2 q_{a2}^2 + \tfrac{1}{2}\gamma_3 q_{a1} q_{a2}$$

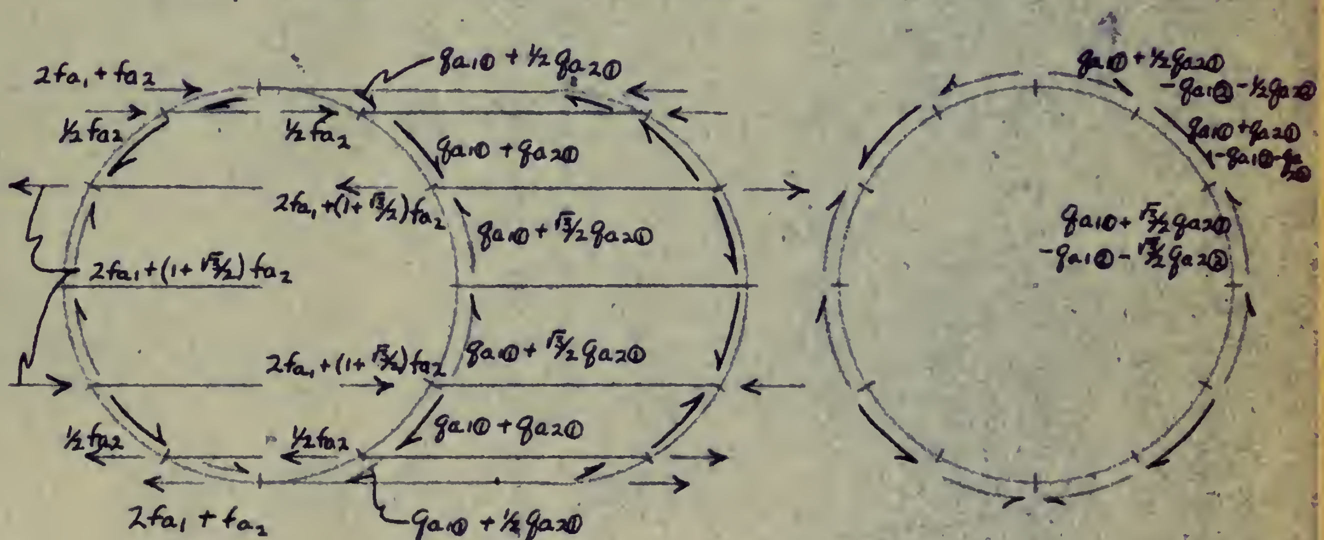

TWELVE STRINGER IDEALIZATION

(S-A)mixed PATTERN

Ring Energy and Sample Bay

$$U_{s12(S-S),\,mixed} = \frac{1}{2}$$

	f_{s1}	f_{s2}	F_{s1}	F_{s2}	$q_{s1(1)}\ell$	$q_{s2(1)}\ell$	$q_{s1(2)}\ell$	$q_{s2(2)}\ell$	$q_{s1(3)}\ell$	$q_{s2(3)}\ell$	$q_{s1(4)}\ell$	$q_{s2(4)}\ell$
f_{s1}	$184m_1 + 6m_2 + \frac{\alpha_1}{\ell^2}$	$2m_2 + \frac{\frac{1}{2}\alpha_3}{\ell^2}$	$8m_1 - 6m_2 - \frac{\alpha_1}{\ell^2}$	$-2m_2 - \frac{\frac{1}{2}\alpha_3}{\ell^2}$	$-86m_1 - 3m_2 - \frac{\frac{1}{2}\alpha_1}{\ell^2}$	$-m_2 - \frac{\frac{1}{4}\alpha_3}{\ell^2}$	$-136m_1 - 6m_2 - \frac{\alpha_1}{\ell^2}$	$-2m_2 - \frac{\frac{1}{2}\alpha_3}{\ell^2}$	$-88m_1 - 6m_2 - \frac{\alpha_1}{\ell^2}$	$-2m_2 - \frac{\frac{1}{2}\alpha_3}{\ell^2}$	$-40m_1 - 6m_2 - \frac{2\alpha_1}{\ell^2}$	$-2m_2 - \frac{\alpha_3}{\ell^2}$
f_{s2}		$92m_1 + 2m_2 + \frac{\alpha_2}{\ell^2}$	$-2m_2 - \frac{\frac{1}{2}\alpha_3}{\ell^2}$	$4m_1 - 2m_2 - \frac{\alpha_2}{\ell^2}$	$-m_2 - \frac{\frac{1}{4}\alpha_3}{\ell^2}$	$-43m_1 - m_2 - \frac{\frac{1}{2}\alpha_2}{\ell^2}$	$-2m_2 - \frac{\frac{1}{2}\alpha_3}{\ell^2}$	$-68m_1 - 2m_2 - \frac{\alpha_2}{\ell^2}$	$-2m_2 - \frac{\frac{1}{2}\alpha_3}{\ell^2}$	$-44m_1 - 2m_2 - \frac{\alpha_2}{\ell^2}$	$-2m_2 - \frac{\alpha_3}{\ell^2}$	$-20m_1 - 2m_2 - \frac{2\alpha_2}{\ell^2}$
F_{s1}			$16m_1 + 6m_2 + \frac{\alpha_1}{\ell^2}$	$2m_2 + \frac{\frac{1}{2}\alpha_3}{\ell^2}$	$-4m_1 + 3m_2 + \frac{\frac{1}{2}\alpha_1}{\ell^2}$	$m_2 + \frac{\frac{1}{4}\alpha_3}{\ell^2}$	$-8m_1 + 6m_2 + \frac{\alpha_1}{\ell^2}$	$2m_2 + \frac{\frac{1}{2}\alpha_3}{\ell^2}$	$-8m_1 + 6m_2 + \frac{\alpha_1}{\ell^2}$	$2m_2 + \frac{\frac{1}{2}\alpha_3}{\ell^2}$	$-8m_1 + 6m_2 + \frac{2\alpha_1}{\ell^2}$	$2m_2 + \frac{\alpha_3}{\ell^2}$
F_{s2}				$8m_1 + 2m_2 + \frac{\alpha_2}{\ell^2}$	$m_2 + \frac{\frac{1}{4}\alpha_3}{\ell^2}$	$-2m_1 + m_2 + \frac{\frac{1}{2}\alpha_2}{\ell^2}$	$2m_2 + \frac{\frac{1}{2}\alpha_3}{\ell^2}$	$-4m_1 + 2m_2 + \frac{\alpha_2}{\ell^2}$	$2m_2 + \frac{\frac{1}{2}\alpha_3}{\ell^2}$	$-4m_1 + 2m_2 + \frac{\alpha_2}{\ell^2}$	$2m_2 + \frac{\alpha_3}{\ell^2}$	$-4m_1 + 2m_2 + \frac{2\alpha_2}{\ell^2}$
$q_{s1(1)}\ell$					$42m_1 + 4\frac{1}{2}m_2 + \frac{\frac{5}{4}\alpha_1}{\ell^2}$	$1\frac{1}{2}m_2 + \frac{\frac{5}{8}\alpha_3}{\ell^2}$	$68m_1 + 3m_2 - \frac{\frac{1}{2}\alpha_1}{\ell^2}$	$m_2 - \frac{\frac{1}{4}\alpha_3}{\ell^2}$	$44m_1 + 3m_2 + \frac{\frac{1}{2}\alpha_1}{\ell^2}$	$m_2 + \frac{\frac{1}{4}\alpha_3}{\ell^2}$	$20m_1 + 3m_2 + \frac{\alpha_1}{\ell^2}$	$m_2 + \frac{\frac{1}{2}\alpha_3}{\ell^2}$
$q_{s2(1)}\ell$						$21m_1 + 1\frac{1}{2}m_2 + \frac{\frac{5}{4}\alpha_2}{\ell^2}$	$m_2 - \frac{\frac{1}{4}\alpha_3}{\ell^2}$	$34m_1 + m_2 - \frac{\frac{1}{2}\alpha_2}{\ell^2}$	$m_2 + \frac{\frac{1}{4}\alpha_3}{\ell^2}$	$22m_1 + m_2 + \frac{\frac{1}{2}\alpha_2}{\ell^2}$	$m_2 + \frac{\frac{1}{2}\alpha_3}{\ell^2}$	$10m_1 + m_2 + \frac{\alpha_2}{\ell^2}$
$q_{s1(2)}\ell$							$128m_1 + 12m_2 + \frac{3\alpha_1}{\ell^2}$	$4m_2 + \frac{\frac{3}{2}\alpha_3}{\ell^2}$	$88m_1 + 6m_2$	$2m_2$	$40m_1 + 6m_2 + \frac{2\alpha_1}{\ell^2}$	$2m_2 + \frac{\alpha_3}{\ell^2}$
$q_{s2(2)}\ell$								$64m_1 + 4m_2 + \frac{3\alpha_2}{\ell^2}$	$2m_2$	$44m_1 + 3m_2$	$2m_2 + \frac{\alpha_3}{\ell^2}$	$20m_1 + 2m_2 + \frac{2\alpha_2}{\ell^2}$
$q_{s1(3)}\ell$									$80m_1 + 12m_2 + \frac{3\alpha_1}{\ell^2}$	$4m_2 + \frac{\frac{3}{2}\alpha_3}{\ell^2}$	$40m_1 + 6m_2 + \frac{\alpha_1}{\ell^2}$	$+2m_2 + \frac{\frac{1}{2}\alpha_3}{\ell^2}$
$q_{s2(3)}\ell$										$40m_1 + 4m_2 + \frac{3\alpha_2}{\ell^2}$	$2m_2 + \frac{\frac{1}{2}\alpha_3}{\ell^2}$	$20m_1 + 2m_2 + \frac{\alpha_2}{\ell^2}$
$q_{s1(4)}\ell$											$32m_1 + 12m_2 + \frac{5\alpha_1}{\ell^2}$	$4m_2 + \frac{\frac{5}{2}\alpha_3}{\ell^2}$
$q_{s2(4)}\ell$												$16m_1 + 4m_2 + \frac{5\alpha_3}{\ell^2}$

$$m_1 = \frac{\ell}{3AE}$$

$$m_2 = \frac{\pi R}{3\ell t G}$$

$U_{s12(s-s)} = \frac{1}{2}$

$m_1 = \frac{\ell}{3AE}$

$m_2 = \frac{\pi R}{3 \ell t G}$

	f_{s3}	F_{s3}	$q_{s3(1)}\ell$	$q_{s3(2)}\ell$	$q_{s3(3)}\ell$	$q_{s3(4)}\ell$
f_{s3}	$276m_1 + 4m_2 + \frac{\beta}{\ell^2}$	$12m_1 - 4m_2 - \frac{\beta}{\ell^2}$	$-129m_1 - 2m_2 - \frac{1/2\,\beta}{\ell^2}$	$-204m_1 - 4m_2 - \frac{\beta}{\ell^2}$	$-132m_1 - 4m_2 - \frac{\beta}{\ell^2}$	$-60m_1 - 4m_2 - \frac{2\beta}{\ell^2}$
F_{s3}		$24m_1 + 4m_2 + \frac{\beta}{\ell^2}$	$-6m_1 + 2m_2 + \frac{1/2\,\beta}{\ell^2}$	$-12m_1 + 4m_2 + \frac{\beta}{\ell^2}$	$-12m_1 + 4m_2 + \frac{\beta}{\ell^2}$	$-12m_1 + 4m_2 + \frac{2\beta}{\ell^2}$
$q_{s3(1)}\ell$			$63m_1 + 3m_2 + \frac{5/4\,\beta}{\ell^2}$	$102m_1 + 2m_2 - \frac{1/2\,\beta}{\ell^2}$	$66m_1 + 2m_2 + \frac{1/2\,\beta}{\ell^2}$	$30m_1 + 2m_2 + \frac{\beta}{\ell^2}$
$q_{s3(2)}\ell$				$192m_1 + 8m_2 + \frac{3\beta}{\ell^2}$	$132m_1 + 4m_2$	$60m_1 + 4m_2 + \frac{2\beta}{\ell^2}$
$q_{s3(3)}\ell$					$120m_1 + 8m_2 + \frac{3\beta}{\ell^2}$	$60m_1 + 4m_2 + \frac{\beta}{\ell^2}$
$q_{s3(4)}\ell$						$48m_1 + 8m_2 + \frac{5\beta}{\ell^2}$

TWELVE STRINGER

(S-S) PATTERN

ENERGY MATRIX

$U_{S12\,(S-A)_{mixed}} = \frac{1}{2}$

	f_{a1}	f_{a2}	F_{a1}	F_{a2}	q_{a1}①l	q_{a2}①l	q_{a1}②l	q_{a2}②l	q_{a1}③l	q_{a2}③l	q_{a1}④l	q_{a2}④l
f_{a1}	$276 m_1 + 6 m_2 + \frac{\gamma_1}{l^2}$	$92(\frac{1}{2}+k)m_1 + (3+\sqrt{3})m_2 + \frac{\frac{1}{2}\gamma_3}{l^2}$	$12 m_1 - 6 m_2 - \frac{\gamma_1}{l^2}$	$4(\frac{1}{2}+k)m_1 - (3+\sqrt{3})m_2 - \frac{\frac{1}{2}\gamma_3}{l^2}$	$-129 m_1 - 3 m_2 - \frac{\frac{1}{2}\gamma_1}{l^2}$	$-43(\frac{1}{2}+k)m_1 - \frac{1}{2}(3+\sqrt{3})m_2 - \frac{\frac{1}{4}\gamma_3}{l^2}$	$-204 m_1 - 6 m_2 - \frac{\gamma_1}{l^2}$	$-68(\frac{1}{2}+k)m_1 - (3+\sqrt{3})m_2 - \frac{\frac{1}{2}\gamma_3}{l^2}$	$-132 m_1 - 6 m_2 - \frac{\gamma_1}{l^2}$	$-44(\frac{1}{2}+k)m_1 - (3+\sqrt{3})m_2 - \frac{\frac{1}{2}\gamma_3}{l^2}$	$-60 m_1 - 6 m_2 - \frac{2\gamma_1}{l^2}$	$-20(\frac{1}{2}+k)m_1 - (3+\sqrt{3})m_2 - \frac{\gamma_3}{l^2}$
f_{a2}		$46(\frac{3}{4}+k^2)m_1 + 4 m_2 + \frac{\gamma_2}{l^2}$	$4(\frac{1}{2}+k)m_1 - (3+\sqrt{3})m_2 - \frac{\frac{1}{2}\gamma_3}{l^2}$	$2(\frac{3}{4}+k^2)m_1 - 4 m_2 - \frac{\gamma_2}{l^2}$	$-43(\frac{1}{2}+k)m_1 - \frac{1}{2}(3+\sqrt{3})m_2 - \frac{\frac{1}{4}\gamma_3}{l^2}$	$-21\frac{1}{2}(\frac{3}{4}+k^2)m_1 - 2 m_2 - \frac{\frac{1}{2}\gamma_2}{l^2}$	$-68(\frac{1}{2}+k)m_1 - (3+\sqrt{3})m_2 - \frac{\frac{1}{2}\gamma_3}{l^2}$	$-34(\frac{3}{4}+k^2)m_1 - 4 m_2 - \frac{\gamma_2}{l^2}$	$-44(\frac{1}{2}+k)m_1 - (3+\sqrt{3})m_1 - \frac{\frac{1}{2}\gamma_3}{l^2}$	$-22(\frac{3}{4}+k^2)m_1 - 4 m_2 - \frac{\gamma_2}{l^2}$	$-20(\frac{1}{2}+k)m_1 - (3+\sqrt{3})m_2 - \frac{\gamma_3}{l^2}$	$-10(\frac{3}{4}+k^2)m_1 - 4 m_2 - \frac{2\gamma_2}{l^2}$
F_{a1}			$24 m_1 + 6 m_2 + \frac{\gamma_1}{l^2}$	$8(\frac{1}{2}+k)m_1 + (3+\sqrt{3})m_2 + \frac{\frac{1}{2}\gamma_3}{l^2}$	$-6 m_1 + 3 m_2 + \frac{\frac{1}{2}\gamma_1}{l^2}$	$-2(\frac{1}{2}+k)m_1 + \frac{1}{2}(3+\sqrt{3})m_2 + \frac{\frac{1}{4}\gamma_3}{l^2}$	$-12 m_1 + 6 m_2 + \frac{\gamma_1}{l^2}$	$-4(\frac{1}{2}+k)m_1 + (3+\sqrt{3})m_2 + \frac{\frac{1}{2}\gamma_3}{l^2}$	$-12 m_1 + 6 m_2 + \frac{\gamma_1}{l^2}$	$-4(\frac{1}{2}+k)m_1 + (3+\sqrt{3})m_2 + \frac{\frac{1}{2}\gamma_3}{l^2}$	$-12 m_1 + 6 m_2 + \frac{2\gamma_1}{l^2}$	$-4(\frac{1}{2}+k)m_1 + (3+\sqrt{3})m_2 + \frac{\gamma_3}{l^2}$
F_{a2}				$4(\frac{3}{4}+k^2)m_1 + 4 m_2 + \frac{\gamma_2}{l^2}$	$-2(\frac{1}{2}+k)m_1 + \frac{1}{2}(3+\sqrt{3})m_2 + \frac{\frac{1}{4}\gamma_3}{l^2}$	$-(\frac{3}{4}+k^2)m_1 + 2 m_2 + \frac{\frac{1}{2}\gamma_2}{l^2}$	$-4(\frac{1}{2}+k)m_1 + (3+\sqrt{3})m_2 + \frac{\frac{1}{2}\gamma_3}{l^2}$	$-2(\frac{3}{4}+k^2)m_1 + 4 m_2 + \frac{\gamma_2}{l^2}$	$-4(\frac{1}{2}+k)m_1 + (3+\sqrt{3})m_2 + \frac{\frac{1}{2}\gamma_3}{l^2}$	$-2(\frac{3}{4}+k^2)m_1 + 4 m_2 + \frac{\gamma_2}{l^2}$	$-4(\frac{1}{2}+k)m_1 + (3+\sqrt{3})m_2 + \frac{\gamma_3}{l^2}$	$-2(\frac{3}{4}+k^2)m_1 + 4 m_2 + \frac{2\gamma_2}{l^2}$
q_{a1}①l					$63 m_1 + 4\frac{1}{2} m_2 + \frac{\frac{5}{4}\gamma_1}{l^2}$	$21(\frac{1}{2}+k)m_1 + \frac{3}{4}(3+\sqrt{3})m_2 + \frac{\frac{5}{8}\gamma_3}{l^2}$	$102 m_1 + 3 m_2 + \frac{\frac{1}{2}\gamma_1}{l^2}$	$34(\frac{1}{2}+k)m_1 + \frac{1}{2}(3+\sqrt{3})m_2 - \frac{\frac{1}{4}\gamma_3}{l^2}$	$66 m_1 + 3 m_2 + \frac{\frac{1}{2}\gamma_1}{l^2}$	$22(\frac{1}{2}+k)m_1 + \frac{1}{2}(3+\sqrt{3})m_2 + \frac{\frac{1}{4}\gamma_3}{l^2}$	$30 m_1 + 3 m_2 + \frac{\gamma_1}{l^2}$	$10(\frac{1}{2}+k)m_1 + \frac{1}{2}(3+\sqrt{3})m_2 + \frac{\frac{1}{2}\gamma_3}{l^2}$
q_{a2}①l						$10\frac{1}{2}(\frac{3}{4}+k^2)m_1 + 3 m_2 + \frac{\frac{5}{4}\gamma_2}{l^2}$	$34(\frac{1}{2}+k)m_1 + \frac{1}{2}(3+\sqrt{3})m_2 - \frac{\frac{1}{4}\gamma_3}{l^2}$	$17(\frac{3}{4}+k^2)m_1 + 2 m_2 - \frac{\frac{1}{2}\gamma_2}{l^2}$	$22(\frac{1}{2}+k)m_1 + \frac{1}{2}(3+\sqrt{3})m_2 + \frac{\frac{1}{4}\gamma_3}{l^2}$	$11(\frac{3}{4}+k^2)m_1 + 2 m_2 + \frac{\frac{1}{2}\gamma_2}{l^2}$	$10(\frac{1}{2}+k)m_1 + \frac{1}{2}(3+\sqrt{3})m_2 + \frac{\frac{1}{2}\gamma_3}{l^2}$	$5(\frac{3}{4}+k^2)m_1 + 2 m_2 + \frac{\gamma_2}{l^2}$
q_{a1}②l							$192 m_1 + 12 m_2 + \frac{3\gamma_1}{l^2}$	$64(\frac{1}{2}+k)m_1 + 2(3+\sqrt{3})m_2 + \frac{\frac{3}{2}\gamma_3}{l^2}$	$132 m_1 + 6 m_2$	$44(\frac{1}{2}+k)m_1 + (3+\sqrt{3})m_2$	$60 m_1 + 6 m_2 + \frac{2\gamma_1}{l^2}$	$20(\frac{1}{2}+k)m_1 + (3+\sqrt{3})m_2 + \frac{\gamma_3}{l^2}$
q_{a2}②l								$32(\frac{3}{4}+k^2)m_1 + 8 m_2 + \frac{3\gamma_2}{l^2}$	$44(\frac{1}{2}+k)m_1 + (3+\sqrt{3})m_2$	$22(\frac{3}{4}+k^2)m_1 + 4 m_2$	$20(\frac{1}{2}+k)m_1 + (3+\sqrt{3})m_2 + \frac{\gamma_3}{l^2}$	$10(\frac{3}{4}+k^2)m_1 + 4 m_2 + \frac{2\gamma_2}{l^2}$
q_{a1}③l									$120 m_1 + 12 m_2 + \frac{3\gamma_1}{l^2}$	$40(\frac{1}{2}+k)m_1 + 2(3+\sqrt{3})m_2 + \frac{\frac{3}{2}\gamma_3}{l^2}$	$60 m_1 + 6 m_2 + \frac{\gamma_1}{l^2}$	$20(\frac{1}{2}+k)m_1 + (3+\sqrt{3})m_2 + \frac{\frac{1}{2}\gamma_3}{l^2}$
q_{a2}③l										$20(\frac{3}{4}+k^2)m_1 + 8 m_2 + \frac{3\gamma_2}{l^2}$	$20(\frac{1}{2}+k)m_1 + (3+\sqrt{3})m_2 + \frac{\frac{1}{2}\gamma_3}{l^2}$	$10(\frac{3}{4}+k^2)m_1 + 4 m_2 + \frac{\gamma_2}{l^2}$
q_{a1}④l											$48 m_1 + 12 m_2 + \frac{5\gamma_1}{l^2}$	$16(\frac{1}{2}+k)m_1 + 2(3+\sqrt{3})m_2 + \frac{\frac{5}{2}\gamma_3}{l^2}$
q_{a2}④l												$8(\frac{3}{4}+k^2)m_1 + 8 m_2 + \frac{5\gamma_2}{l^2}$

$m_1 = \frac{l}{3AE}$

$m_2 = \frac{\pi R}{3 l t G}$

$k = 1 + \frac{1}{2}\sqrt{3}$

II. CONCLUSIONS

It was originally hoped that this thesis would provide the basis for a standardized method of preliminary stress analysis for the type of structure with which it is concerned. Disregarding, for the moment, the comparison plots of Appendix II, the application and advantages of the method will first be discussed.

Even though the simplicity of the idealization precludes great accuracy, this analysis can be used in preliminary design to provide a relatively quick check on the adequacy of the structure. When the design becomes finalized, a detailed check, using one of the more accurate methods of stress analysis (e.g. that presented in reference (3)) or using an experimental model, may be made.

In the exact form contained herein, the analysis should be applied only to a nine bay structure with load axis thru stringers and cutout in the center or center plus symmetrically placed adjacent bays. A structural analyst would be required to set up the boundary equations defined by the physical structure and to derive the elimination matrix, but the calculations of matrix factors for computer use and transcription of results can be accomplished by less highly trained personnel. The physical parameters (i.e. those items underlined on table IV - 1,

page (16) may be varied without rederiving the elimination matrix so that a check on redesign may be rapidly made.

The method of analysis may also be used to obtain results corresponding to structures which vary in number of bays from that assumed in the thesis. Furthermore, by "tagging" parameters from a given bay, an analysis may be made of a structure in which physical parameters vary from bay to bay, such as changes in stringer cross sections. Finally non-cutout cases may be handled by combining the idealizations properly.

The major objection to the above which may be cited is the evidence of poor agreement with experimental results seen in Appendix II. In spite of these somewhat disappointing results, it is felt that the obvious advantages warrant a more thorough check than time permitted. It would be especially interesting to have experimental stress data in the 180 degree area where the twelve stringer idealization predicts a minimum of compression (the reversal to slight tension actually computed for one of the bays is considered highly unlikely).

In summary, it is felt that, even with its relatively poor agreement with the only experimental data available, the analysis presented herein could be profitably used in preliminary design to quickly obtain approximate structural

scantlings. Further, the possible advantages seem to the author to warrant an experimental model set up specifically to verify the analytical data and an investigation of the effect of minor changes in analysis.

REFERENCES

1. Jensen, W. R.: "On Simplified Fuselage-Structure Stress Distributions." Journal of the Aero/Space Sciences, vol. 25, no. 10, Oct. 1958, pp. 656-657.

2. Schlechte, Floyd R., and Rosencrans, Richard: Experimental Stress Analysis of Stiffened Cylinders with Cutouts, Pure Bending. NACA TN 3073, 1954.

3. McComb, Harvey G., Jr.: Stress Analysis of Circular Semimonocoque Cylinders with Cutouts by a Perturbation Load Technique. NACA TN 3200, 1954.

4. McComb, Harvey G., Jr., and Low, Emmet F., Jr.: Tables of Coefficients for the Analysis of Stresses about Cutouts in Circular Semimonocoque Cylinders with Flexible Rings. NACA TN 3460, 1955.

5. McComb, Harvey G., Jr., and Low, Emmet F., Jr.: Comparison Between Theoretical and Experimental Stresses in Circular Semimonocoque Cylinders with Rectangular Cutouts. NACA TN 3544, 1955.

6. Aitken, A. C.: Determinants and Matrices. New York: Interscience Publishers, Inc., 1949. 144 pp.

7. Wehle, L. B., Jr., and Lansing, Warner: "A Method for Reducing the Analysis of Complex Redundant Structures to a Routine Procedure." Journal of the Aeronautical Sciences, vol. 19, no. 10, Oct. 1952, pp. 677-684.

APPENDIX I

DETAILED ANALYSIS OF SIX STRINGER (S-S) PATTERN

I. AVAILABLE RING PATTERNS

Figure AI - 1 illustrates the only three possible independent ring shear patterns for this idealization. The total number of such patterns is fixed by the three static stability conditions at six minus three equals three. An (A-S) pattern is not possible because a horizontal symmetry axis requires zero shear on the side panels while a vertical antisymmetry axis requires a continuity of shear across the upper and lower pairs of panels. With these conditions it is not possible to satisfy both

$$\Sigma F_H = 0$$

and

$$\Sigma M = 0.$$

Since the load pattern requires a vertical symmetry axis, only the (S-S) and (S-A) shear patterns are available.

Figure AI - 1

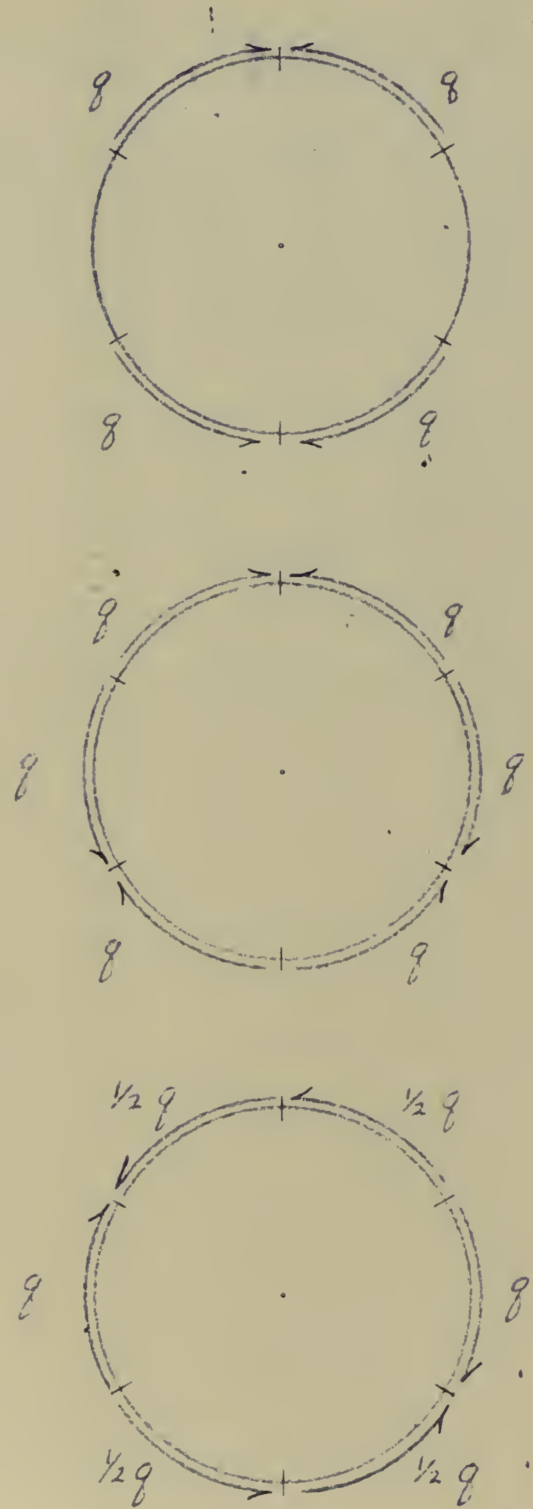

(S-S)

(S-A)

(A-A)

SIX STRINGER RING PATTERNS

II. (S-S) STRUCTURE ANALYSIS

Figure AI - 2 and its accompanying calculations illustrate the procedure for finding the bay energy as the sum of the energies of the elements (i.e. ring, panels, and stringers).

Figures AI - 3 thru AI -7 with tables AI - 1 thru AI - 5 illustrate the procedure for finding the successive bay energies. Table AI - 6 represents the total structure energy and is the sum in each matrix block, of the corresponding blocks in the matrices of each bay.

Figure AI - 2

SAMPLE BAY ENERGY CALCULATION

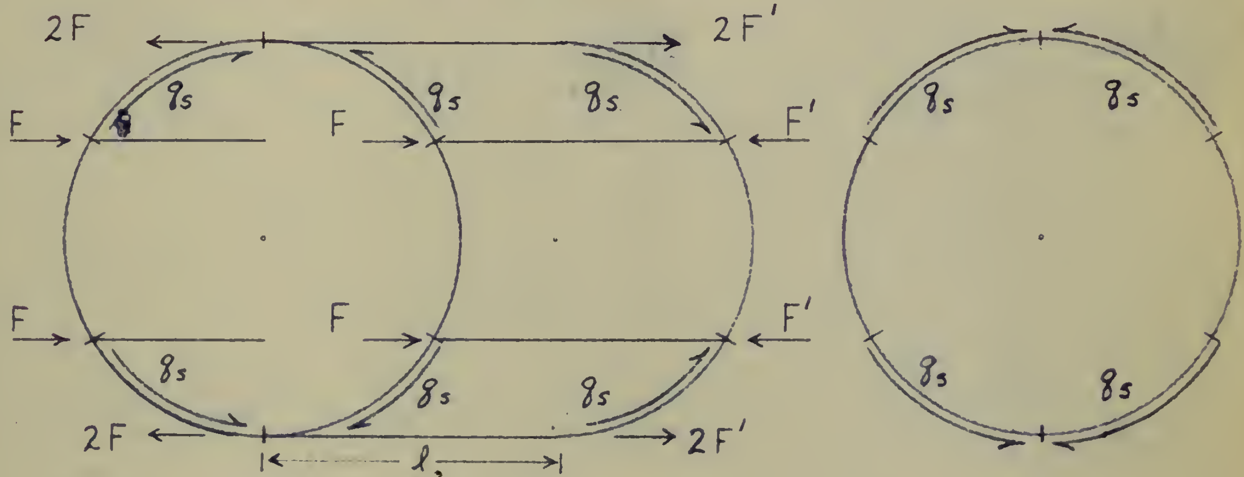

RING ENERGY

$$U_R = \tfrac{1}{2}\beta_1 q_s^2 = \tfrac{1}{2}\frac{\beta_1}{l^2}(q_s l)^2$$

PANEL ENERGY

$$U_P = 4\left[\tfrac{1}{2}\left\{q_s^2 \ \frac{\pi R}{3} \ l \ \frac{1}{Gt}\right\}\right] = \tfrac{1}{2}\ \frac{4\pi R}{3ltG}\ (q_s l)^2$$

STRINGER ENERGY

$$U_S = 2\left[\tfrac{1}{2}\frac{l}{3AE}\left(4F^2 + 4FF' + 4F'^2\right)\right] + 4\left[\tfrac{1}{2}\frac{l}{3AE}\left(F^2 + FF' + F'^2\right)\right]$$

$$= \tfrac{1}{2}\left[\frac{4l}{AE}\left(F^2 + FF' + F'^2\right)\right]$$

BAY ENERGY

$$U_B = U_R + U_P + U_S$$

$$= \tfrac{1}{2}\left[\left\{\frac{\beta_1}{l^2} + \frac{4\pi R}{3ltG}\right\}(q_s l)^2 + \left\{\frac{4l}{AE}\right\}\left(F^2 + FF' + F'^2\right)\right]$$

NOTE: In normal bays, $F' = F - q_s l$

Figure AI - 3

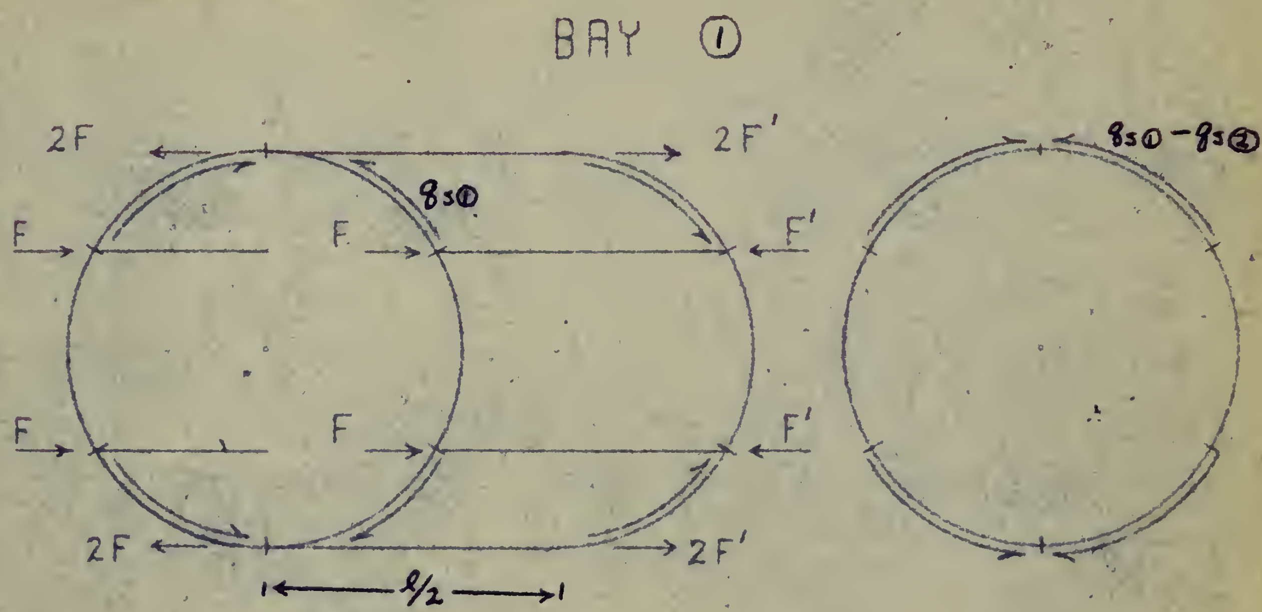

$$F = f_s$$

$$F' = f_s - \tfrac{1}{2} q_{s1} l$$

SIX STRINGER (S-S) PATTERN

Table AI -1

	f_s	F_s	$q_{s\textcircled{1}}\ell$	$q_{s\textcircled{2}}\ell$	$q_{s\textcircled{3}}\ell$	$q_{s\textcircled{4}}\ell$
f_s	$\frac{6\ell}{AE}$		$-\frac{3\ell}{2AE}$			
F_s						
$q_{s\textcircled{1}}\ell$			$\frac{\ell}{2AE} + \frac{2\pi R}{3\ell tG} + \frac{\beta_1}{\ell^2}$	$-\frac{\beta_1}{\ell^2}$		
$q_{s\textcircled{2}}\ell$				$\frac{\beta_1}{\ell^2}$		
$q_{s\textcircled{3}}\ell$						
$q_{s\textcircled{4}}\ell$						

$U_{B\textcircled{1}6}(s\text{-}s) = \frac{1}{2}$

SIX STRINGER

(S-S) PATTERN

BAY ENERGY

Figure AI - 4

BAY 2

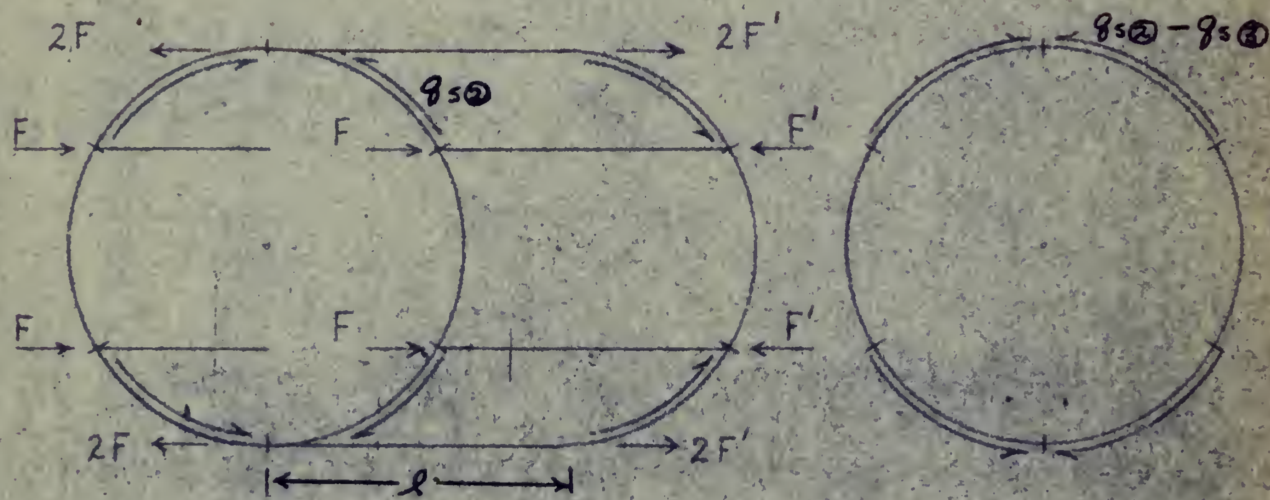

$F = f_s - \frac{1}{2} q_{s1} l$

$F' = f_s - \frac{1}{2} q_{s1} l - q_{s2} l$

SIX STRINGER (S-S) PATTERN

Table AI -2

	f_s	F_s	$q_{s①}\ell$	$q_{s②}\ell$	$q_{s③}\ell$	$q_{s④}\ell$
f_s	$\frac{12\ell}{AE}$		$\frac{-6\ell}{AE}$	$-\frac{6\ell}{AE}$		
F_s						
$q_{s①}\ell$			$\frac{3\ell}{AE}$	$\frac{3\ell}{AE}$		
$q_{s②}\ell$				$\frac{4\ell}{AE} + \frac{4\pi R}{3\ell tG} + \frac{\beta_1}{\ell^2}$	$-\frac{\beta_1}{\ell^2}$	
$q_{s③}\ell$					$\frac{\beta_1}{\ell^2}$	
$q_{s④}\ell$						

$U_{B②6(s\text{-}s)} = \frac{1}{2}$

SIX STRINGER

(S-S) PATTERN

BAY ENERGY

Figure AI - 5

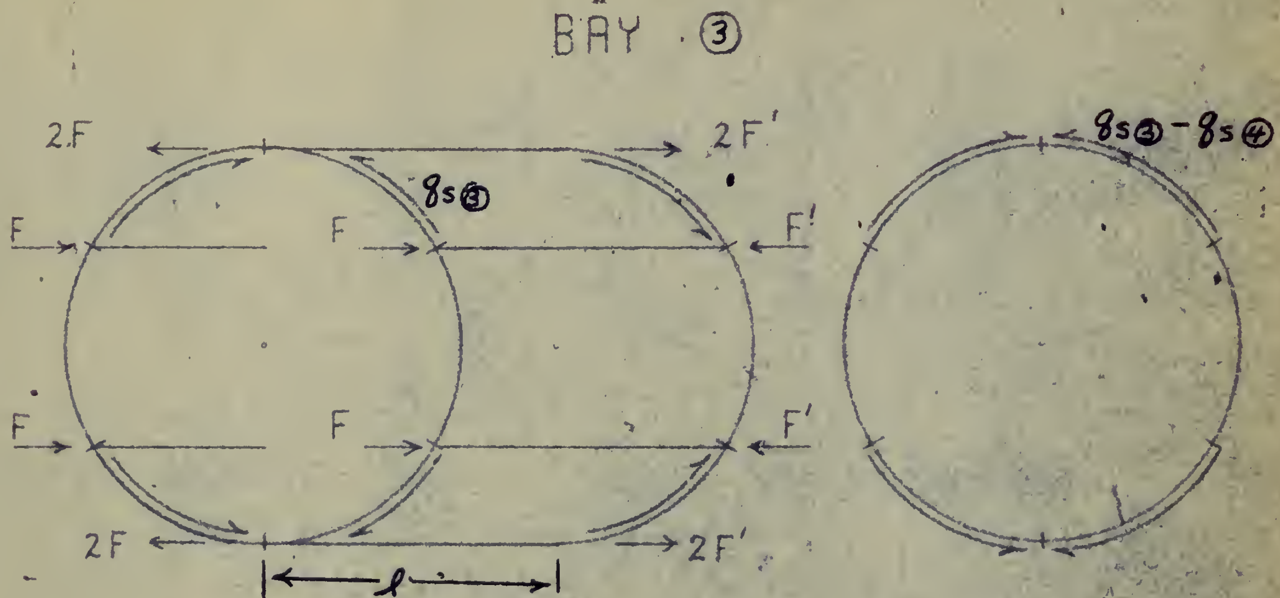

$$F = f_s - \tfrac{1}{2}\, q_{s①}\ell - q_{s②}\ell$$

$$F' = f_s - \tfrac{1}{2}\, q_{s①}\ell - q_{s②}\ell - q_{s③}\ell$$

SIX STRINGER (S-S) PATTERN

Table AI - 3

	f_s	F_s	$g_{s①}\ell$	$g_{s②}\ell$	$g_{s③}\ell$	$g_{s④}\ell$
f_s	$\frac{12\ell}{AE}$		$\frac{-6\ell}{AE}$	$-\frac{12\ell}{AE}$	$-\frac{6\ell}{AE}$	
F_s						
$g_{s①}\ell$			$\frac{3\ell}{AE}$	$\frac{6\ell}{AE}$	$\frac{3\ell}{AE}$	
$g_{s②}\ell$				$\frac{12\ell}{AE}$	$\frac{6\ell}{AE}$	
$g_{s③}\ell$					$\frac{4\ell}{AE}+\frac{4\pi R}{3\ell tG}+\frac{\beta_1}{\ell^2}$	$-\frac{\beta_1}{\ell^2}$
$g_{s④}\ell$						$\frac{\beta_1}{\ell^2}$

$U_{B③6}(s\text{-}s) = \frac{1}{2}$

SIX STRINGER

(S-S) PATTERN

BAY ENERGY

Figure AI - 6

BAY ④

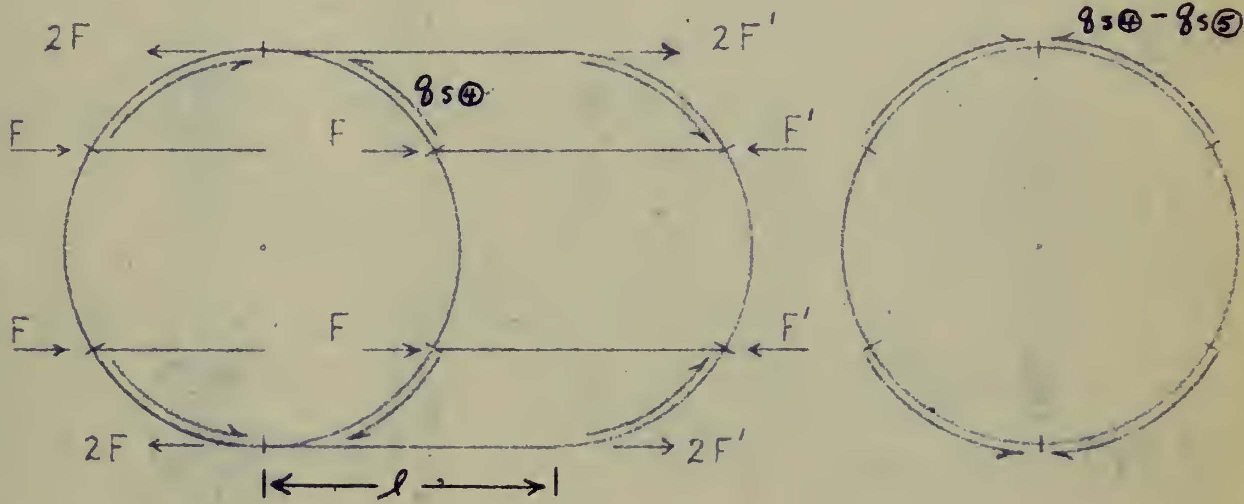

$$F = f_s - \tfrac{1}{2} q_{s①} l - q_{s②} l - q_{s③} l$$

$$F' = f_s - \tfrac{1}{2} q_{s①} l - q_{s②} l - q_{s③} l - q_{s④} l$$

$$q_{s5} = \frac{f_s - F_s}{l} - \tfrac{1}{2} q_{s①} l - q_{s②} l - q_{s③} l - q_{s④} l$$

(see Bay ⑤)

SIX STRINGER (S-S) PATTERN

Table AI - 4

SIX STRINGER

(S-S) PATTERN

BAY ENERGY

$U_{B④(s-s)} = \frac{1}{2}$

	f_s	F_s	$q_{s1}\ell$	$q_{s2}\ell$	$q_{s3}\ell$	$q_{s4}\ell$
f_s	$\frac{12\ell}{AE}+\frac{\beta_1}{\ell^2}$	$-\frac{\beta_1}{\ell^2}$	$-\frac{6\ell}{AE}-\frac{\beta_1}{2\ell^2}$	$-\frac{12\ell}{AE}-\frac{\beta_1}{\ell^2}$	$-\frac{12\ell}{AE}-\frac{\beta_1}{\ell^2}$	$-\frac{6\ell}{AE}-\frac{2\beta_1}{\ell^2}$
F_s		$\frac{\beta_1}{\ell^2}$	$\frac{\beta_1}{2\ell^2}$	$\frac{\beta_1}{\ell^2}$	$\frac{\beta_1}{\ell^2}$	$\frac{2\beta_1}{\ell^2}$
$q_{s1}\ell$			$\frac{3\ell}{AE}+\frac{\beta_1}{4\ell^2}$	$\frac{6\ell}{AE}+\frac{\beta_1}{2\ell^2}$	$\frac{6\ell}{AE}+\frac{\beta_1}{2\ell^2}$	$\frac{3\ell}{AE}+\frac{\beta_1}{\ell^2}$
$q_{s2}\ell$				$\frac{12\ell}{AE}+\frac{\beta_1}{\ell^2}$	$\frac{12\ell}{AE}+\frac{\beta_1}{\ell^2}$	$\frac{6\ell}{AE}+\frac{2\beta_1}{\ell^2}$
$q_{s3}\ell$					$\frac{12\ell}{AE}+\frac{\beta_1}{\ell^2}$	$\frac{6\ell}{AE}+\frac{2\beta_1}{\ell^2}$
$q_{s4}\ell$						$\frac{4\ell}{AE}+\frac{4\pi R}{3\ell tG}+\frac{4\beta_1}{\ell^2}$

Figure AI -7

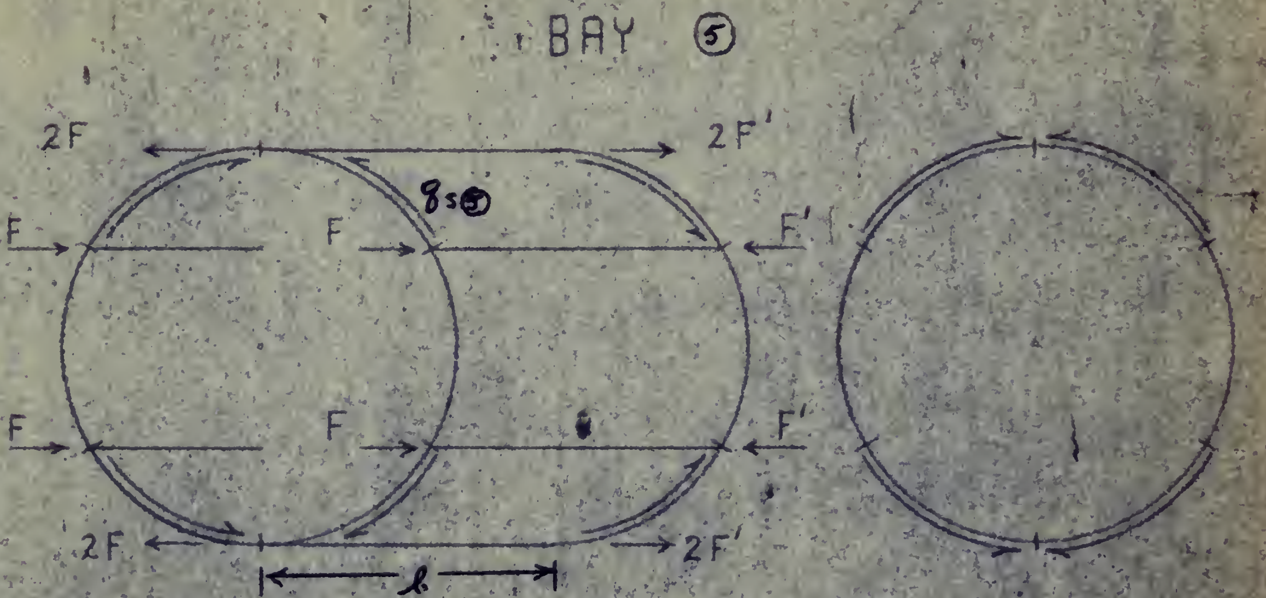

$$F = f_s - \tfrac{1}{2} q_{s①}\ell - q_{s②}\ell - q_{s③}\ell - q_{s④}\ell$$

$$F' = F_s$$

$$q_{s⑤} = \frac{f_s - F_s}{\ell} - \tfrac{1}{2} q_{s①}\ell - q_{s②}\ell - q_{s③}\ell - q_{s④}\ell$$

The final ring is considered built into rigid structure, ∴ $I \to \infty$ and $\beta_1 = 0$.

SIX STRINGER (S-S) PATTERN

Table AI -5

	f_s	F_s	$g_{s1}\ell$	$g_{s2}\ell$	$g_{s3}\ell$	$g_{s4}\ell$
f_s	$\frac{4\ell}{AE}+\frac{4\pi R}{3\ell tG}$	$\frac{2\ell}{AE}-\frac{4\pi R}{3\ell tG}$	$-\frac{2\ell}{AE}-\frac{2\pi R}{3\ell tG}$	$-\frac{4\ell}{AE}-\frac{4\pi R}{3\ell tG}$	$-\frac{4\ell}{AE}-\frac{4\pi R}{\ell tG}$	$-\frac{4\ell}{AE}-\frac{4\pi R}{3\ell tG}$
F_s		$\frac{4\ell}{AE}+\frac{4\pi R}{3\ell tG}$	$-\frac{\ell}{AE}+\frac{2\pi R}{3\ell tG}$	$-\frac{2\ell}{AE}+\frac{4\pi R}{3\ell tG}$	$-\frac{2\ell}{AE}+\frac{4\pi R}{3\ell tG}$	$-\frac{2\ell}{AE}+\frac{4\pi R}{3\ell tG}$
$g_{s1}\ell$			$\frac{\ell}{AE}+\frac{\pi R}{3\ell tG}$	$\frac{2\ell}{AE}+\frac{2\pi R}{3\ell tG}$	$\frac{2\ell}{AE}+\frac{2\pi R}{3\ell tG}$	$\frac{2\ell}{AE}+\frac{2\pi R}{3\ell tG}$
$g_{s2}\ell$				$\frac{4\ell}{AE}+\frac{4\pi R}{3\ell tG}$	$\frac{4\ell}{AE}+\frac{4\pi R}{3\ell tG}$	$\frac{4\ell}{AE}+\frac{4\pi R}{3\ell tG}$
$g_{s3}\ell$					$\frac{4\ell}{AE}+\frac{4\pi R}{3\ell tG}$	$\frac{4\ell}{AE}+\frac{4\pi R}{3\ell tG}$
$g_{s4}\ell$						$\frac{4\ell}{AE}+\frac{4\pi R}{3\ell tG}$

$$U_{B56(S-S)} = \frac{1}{2}$$

SIX STRINGER

(S-S) PATTERN

BAY ENERGY

Table AI - 6

SIX STRINGER

(S-S) PATTERN

STRUCTURE ENERGY

$U_{S6(S-S)} = \frac{1}{2}$

	f_s	F_s	$g_{s①}\ell$	$g_{s②}\ell$	$g_{s③}\ell$	$g_{s④}\ell$
f_s	$\frac{4\pi R}{3\ell tG} + \frac{46\ell}{AE} + \frac{\beta_1}{\ell^2}$	$-\frac{4\pi R}{3\ell tG} + \frac{2\ell}{AE} - \frac{\beta_1}{\ell^2}$	$-\frac{2\pi R}{3\ell tG} - \frac{43\ell}{2AE} - \frac{\beta_1}{2\ell^2}$	$-\frac{4\pi R}{3\ell tG} - \frac{34\ell}{AE} - \frac{\beta_1}{\ell^2}$	$-\frac{4\pi R}{3\ell tG} - \frac{22\ell}{AE} - \frac{\beta_1}{\ell^2}$	$-\frac{4\pi R}{3\ell tG} - \frac{10\ell}{AE} - \frac{2\beta_1}{\ell^2}$
F_s		$\frac{4\pi R}{3\ell tG} + \frac{4\ell}{4E} + \frac{\beta_1}{\ell^2}$	$\frac{2\pi R}{3\ell tG} - \frac{\ell}{AE} + \frac{\beta_1}{2\ell^2}$	$\frac{4\pi R}{3\ell tG} - \frac{2\ell}{AE} + \frac{\beta_1}{\ell^2}$	$\frac{4\pi R}{3\ell tG} - \frac{2\ell}{AE} + \frac{\beta_1}{\ell^2}$	$\frac{4\pi R}{3\ell tG} - \frac{2\ell}{AE} + \frac{2\beta_1}{\ell^2}$
$g_{s①}\ell$			$\frac{3\pi R}{3\ell tG} + \frac{21\ell}{2AE} + \frac{5\beta_1}{4\ell^2}$	$\frac{2\pi R}{3\ell tG} + \frac{17\ell}{AE} - \frac{\beta_1}{2\ell^2}$	$\frac{2\pi R}{3\ell tG} + \frac{11\ell}{AE} + \frac{\beta_1}{2\ell^2}$	$\frac{2\pi R}{3\ell tG} + \frac{5\ell}{AE} + \frac{\beta_1}{\ell^2}$
$g_{s②}\ell$				$\frac{8\pi R}{3\ell tG} + \frac{32\ell}{AE} + \frac{3\beta_1}{\ell^2}$	$\frac{4\pi R}{3\ell tG} + \frac{22\ell}{AE}$	$\frac{4\pi R}{3\ell tG} + \frac{10\ell}{AE} + \frac{2\beta_1}{\ell^2}$
$g_{s③}\ell$					$\frac{8\pi R}{3\ell tG} + \frac{20\ell}{AE} + \frac{3\beta_1}{\ell^2}$	$\frac{4\pi R}{3\ell tG} + \frac{10\ell}{AE} + \frac{\beta_1}{\ell^2}$
$g_{s④}\ell$						$\frac{8\pi R}{3\ell tG} + \frac{8\ell}{AE} + \frac{5\beta_1}{\ell^2}$

APPENDIX II

COMPARISON WITH EXPERIMENTAL RESULTS

I. COMPARISON STRUCTURE AND PROCEDURE

Reference (3) presents the stress data obtained by loading, in pure bending, an experimental cylindrical semimonocoque shell in which a centrally located cutout of varying circumferential length had been made. These data were chosen as the most readily available check on the validity of the practical application of this analysis. Accordingly, the physical constants and combination equations necessary to make each analytical idealization conform to the experimental structure were derived. The combined matrices for each idealization were solved for redundants on an IBM 650 computor. From the redundant solutions, the stringer stress values at several stations along the cylinder were computed. For each such station a plot was made of analytical and experimental stress values versus angular position. The zero angle position was vertically downward, figure AII - 1.

Because ring and skin shear values in the analytical structure are constant between stringer positions and because the angular extent of such values is so much

larger than in the experimental structure, it was felt that plots of these quantities would not be particularly informative. An exception to this is the eight stringer case where, because the idealization provided a cutout size identical to that of an experimental structure, panel shear comparisons were made for the bay containing the cutout.

Before the comparison results are presented, three qualifying points should be noted:

1. The axis load symmetry in the experimental structure is placed thru the center of panels. All analytical results were obtained by placing this axis thru stringer points - points of natural shear discontinuity.
2. In both the six and twelve stringer idealizations, the cutout size used was 120 degrees. The closest experimental data are for a 130 degree cutout.
3. The moment is so applied to the structure that the cutout side is in tension. The same numerical value of moment is considered to be applied to the idealized structure as was applied to the physical structure.

Figure AII - 1

SIGN CONVENTION FOR THETA

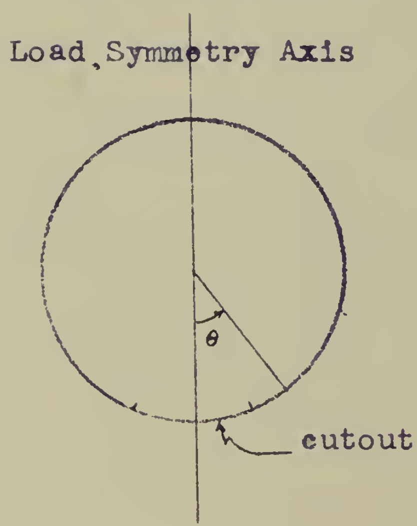

II. SIX STRINGER COMPARISON

The application of a particular idealization to a moment loaded physical structure is accomplished by combining the various symmetry patterns with the moment induced stringer loads so that the loads acting on cutaway structure are iliminated. In the six stringer case, with a 120 degree cutout, the superposition yields the following equations:

1. $(2f_a - 2q_{a①}\, b/2) - (2f_s - 2q_{s①}\, b/2) - F_m = 0$

2. $q_{s①} - q_{s②} = 0$

Fm is the moment induced tension load in the bottom stringer and equation 1. is derived from the requirement that this stringer have a zero load at each end of the middle bay. Equation 2. imposes a zero shear load on the panels on either side of the bottom stringer in bay 1.

The combination equations are used to eliminate redundants from the matrix which results from the superposition of the pattern matrices. These equations also introduce the applied moment in the form of Fm. For the six stringer case the final combination equations are:

1. $f_s = f_a - \frac{1}{2} F_m$

2. $q_{s①} = q_{a①}$

Figures AII - 2, 3, and 4 give the comparison plots with reference data for the 130 degree cutout.

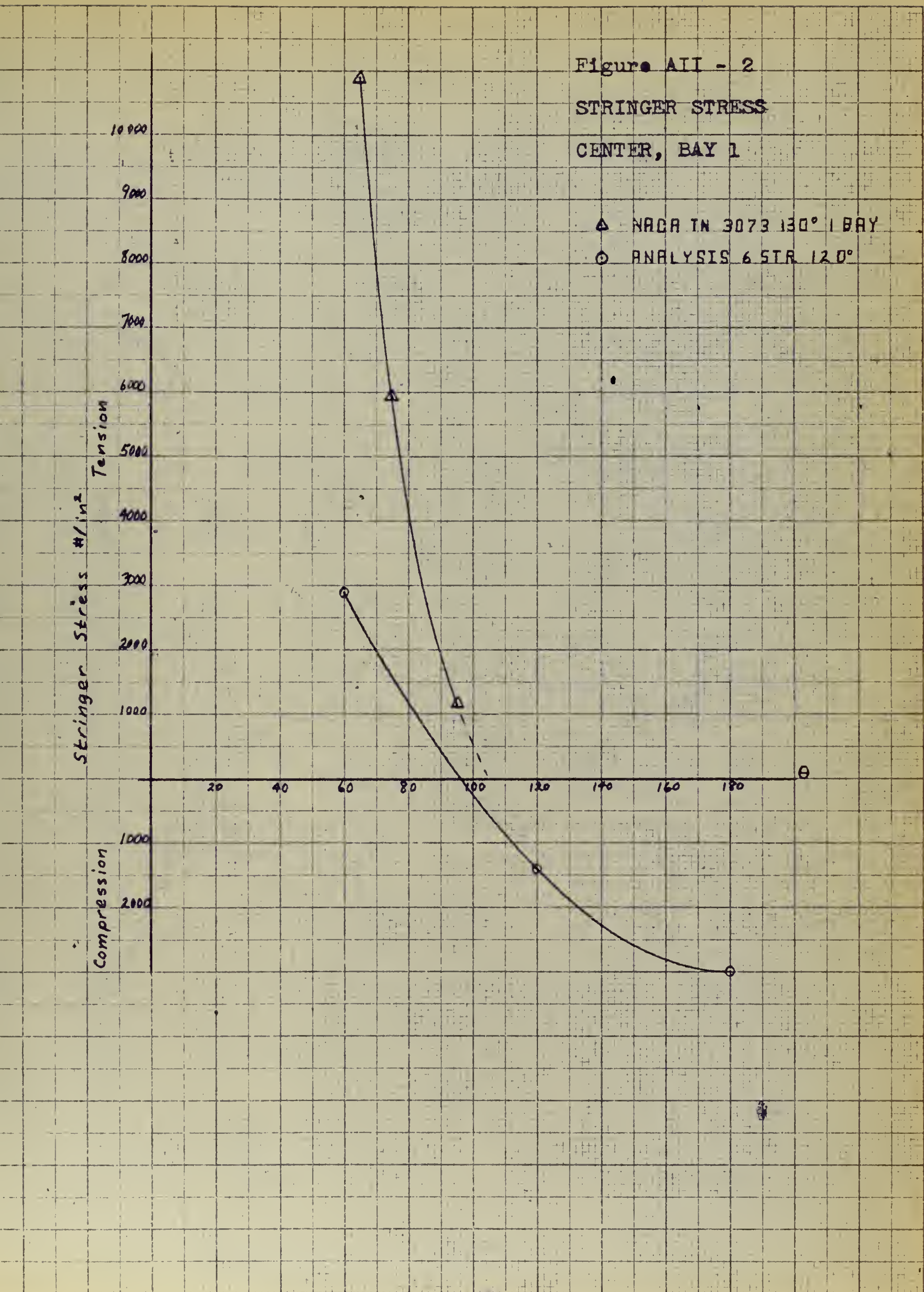

Figure AII - 2
STRINGER STRESS
CENTER, BAY 1
NACA TN 3073 130° 1 BAY
ANALYSIS 6 STR 120°
Stringer Stress #/in²
Tension
Compression
10000
9000
8000
7000
6000
5000
4000
3000
2000
1000
1000
2000
20
40
60
80
100
120
140
160
180
θ

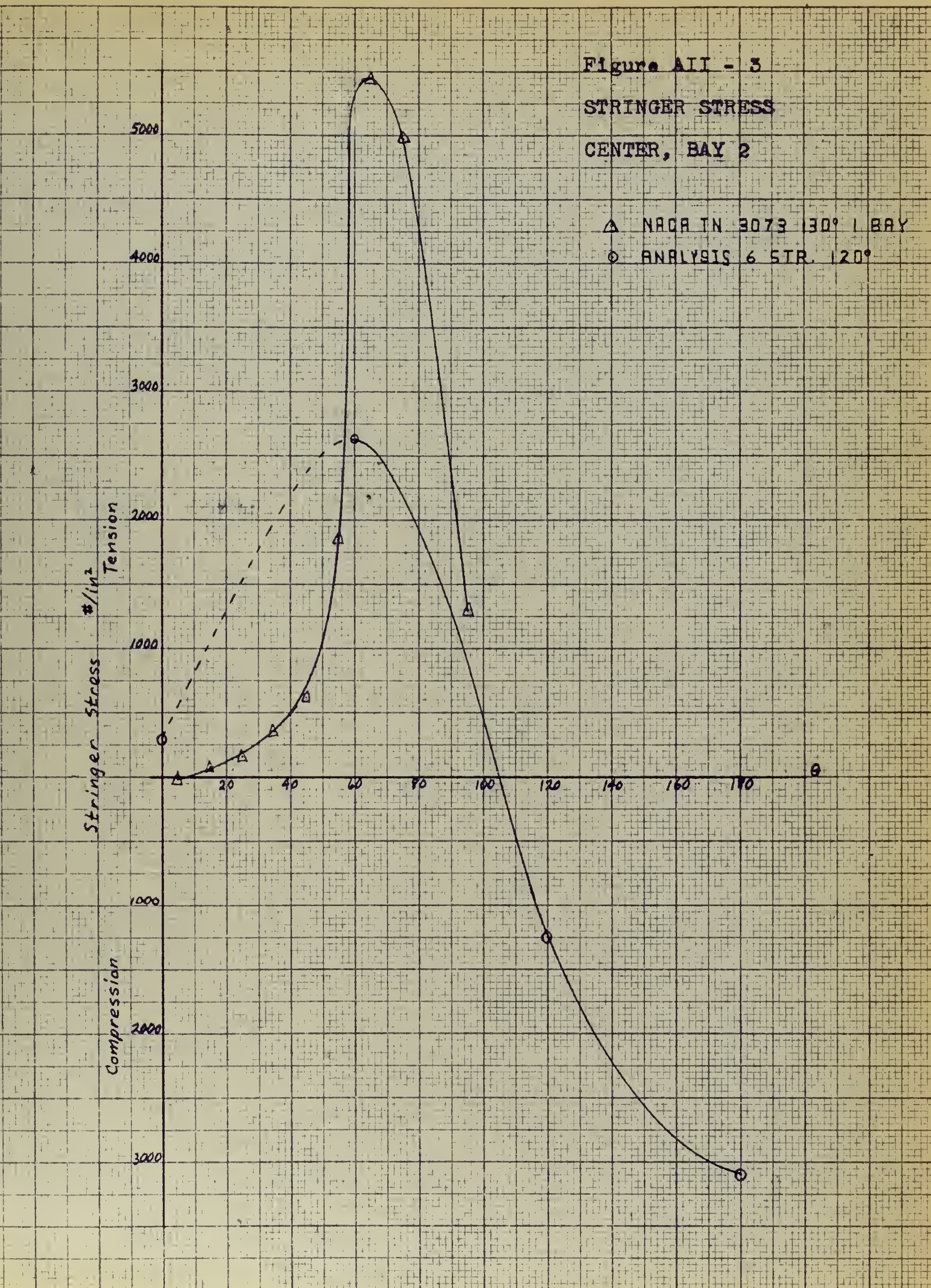

Figure AII - 3
STRINGER STRESS
CENTER, BAY 2
NACA TN 3073 130° 1 BAY
ANALYSIS 6 STR. 120°
5000
4000
3000
2000
1000
1000
2000
3000
Stringer Stress #/in²
Tension
Compression
20
40
60
80
100
120
140
160
180
θ

Figure AII -4

STRINGER STRESS

CENTER, BAY 3

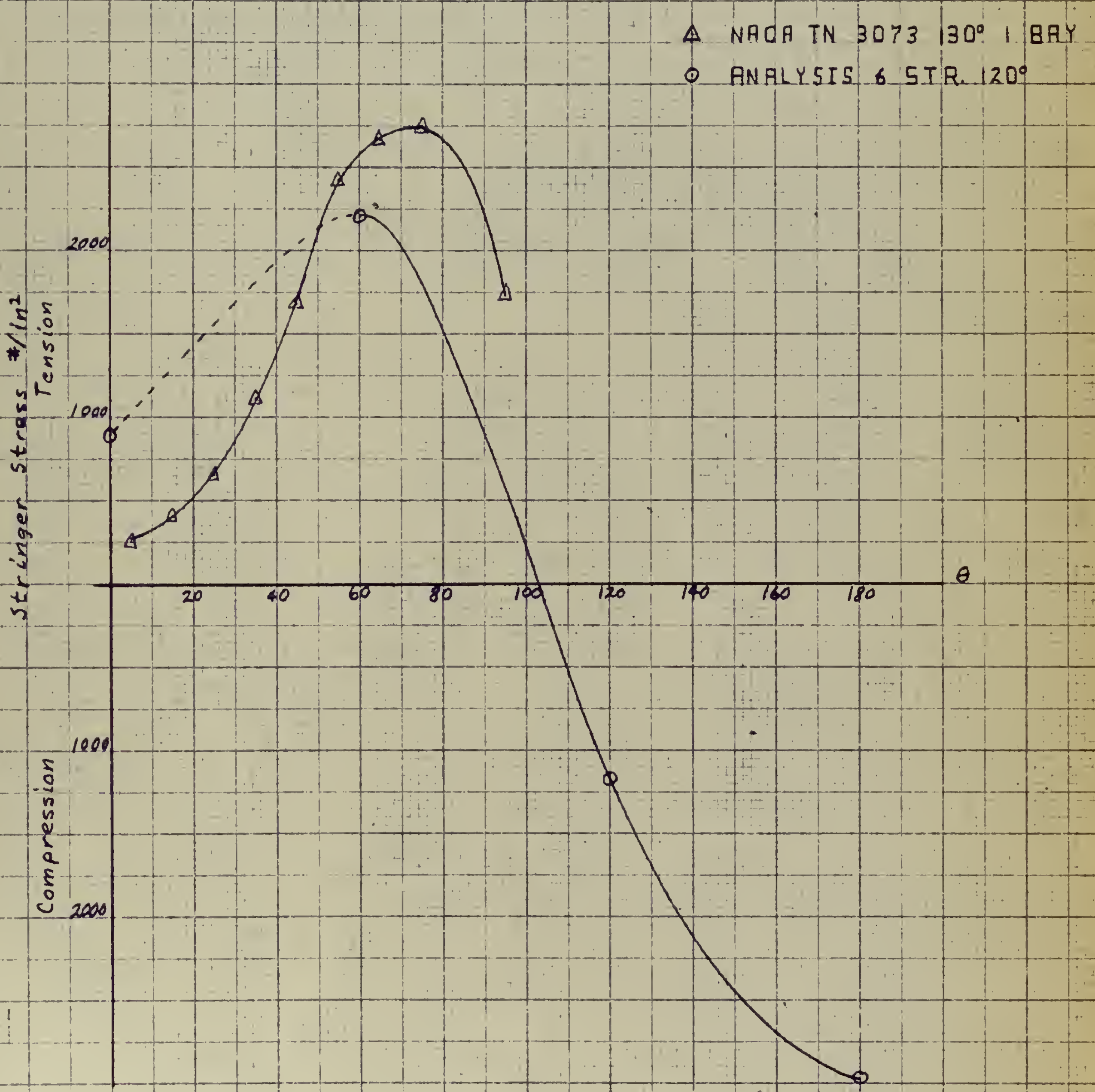

III. EIGHT STRINGER COMPARISON

The three patterns must be superimposed with the applied moment to produce zero load in the bottom stringer and zero shear in the two adjacent panels. The following two elimination equations result.

1. $f_{s1} = f_{s2} - f_a - \frac{1}{2} F_m$

2. $q_{s1 ① l} = q_{s2 ① l} - q_{a1 ① l}$

Figures AII - 5, 6, 7, and 8 give the comparison plots with reference data for the 90 degree cutout.

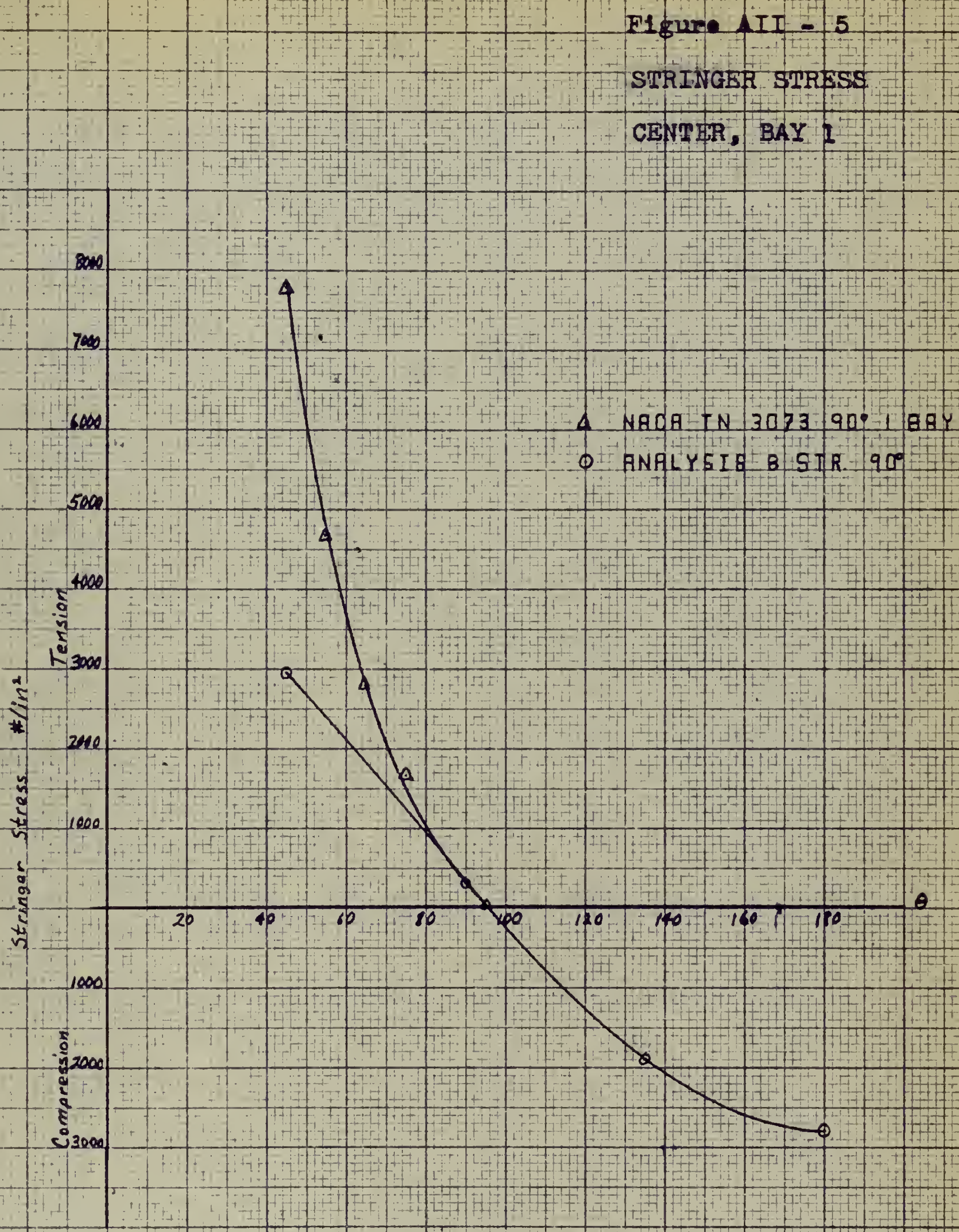

Figure AII - 5
STRINGER STRESS
CENTER, BAY 1
Δ NACA TN 3073 90° 1 BAY
O ANALYSIS 8 STR. 90°
Stringer Stress #/in²
Tension
Compression
8000
7000
6000
5000
4000
3000
2000
1000
1000
2000
3000
20
40
60
80
100
120
140
160
180
θ

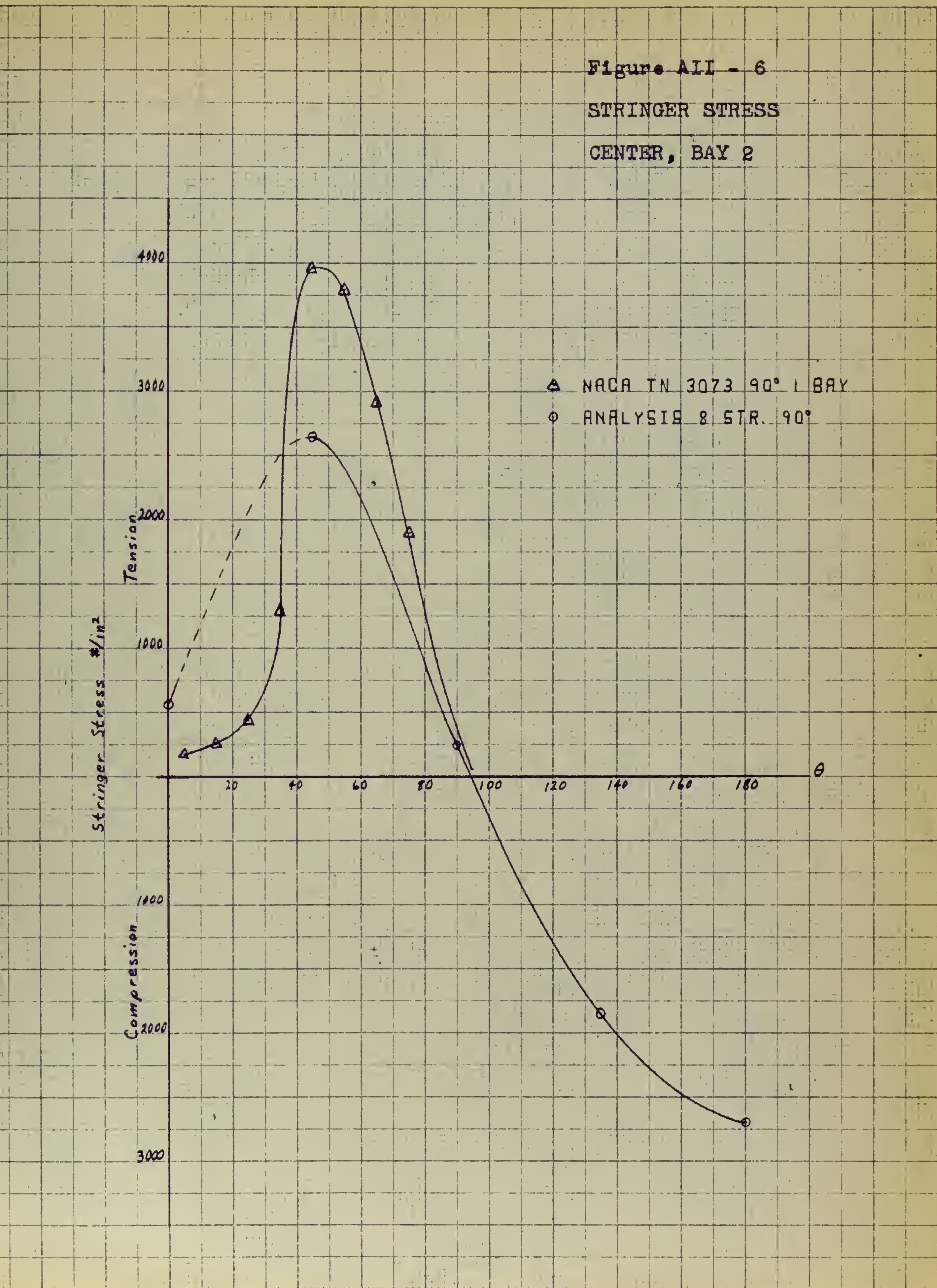
Figure AII - 6
STRINGER STRESS
CENTER, BAY 2
NACA TN 3073 90° 1 BAY
ANALYSIS 8 STR. 90°
Stringer Stress #/in²
Tension
Compression
4000
3000
2000
1000
1000
2000
3000
20
40
60
80
100
120
140
160
180
θ

Figure AII - 7

STRINGER STRESS

CENTER, BAY 3

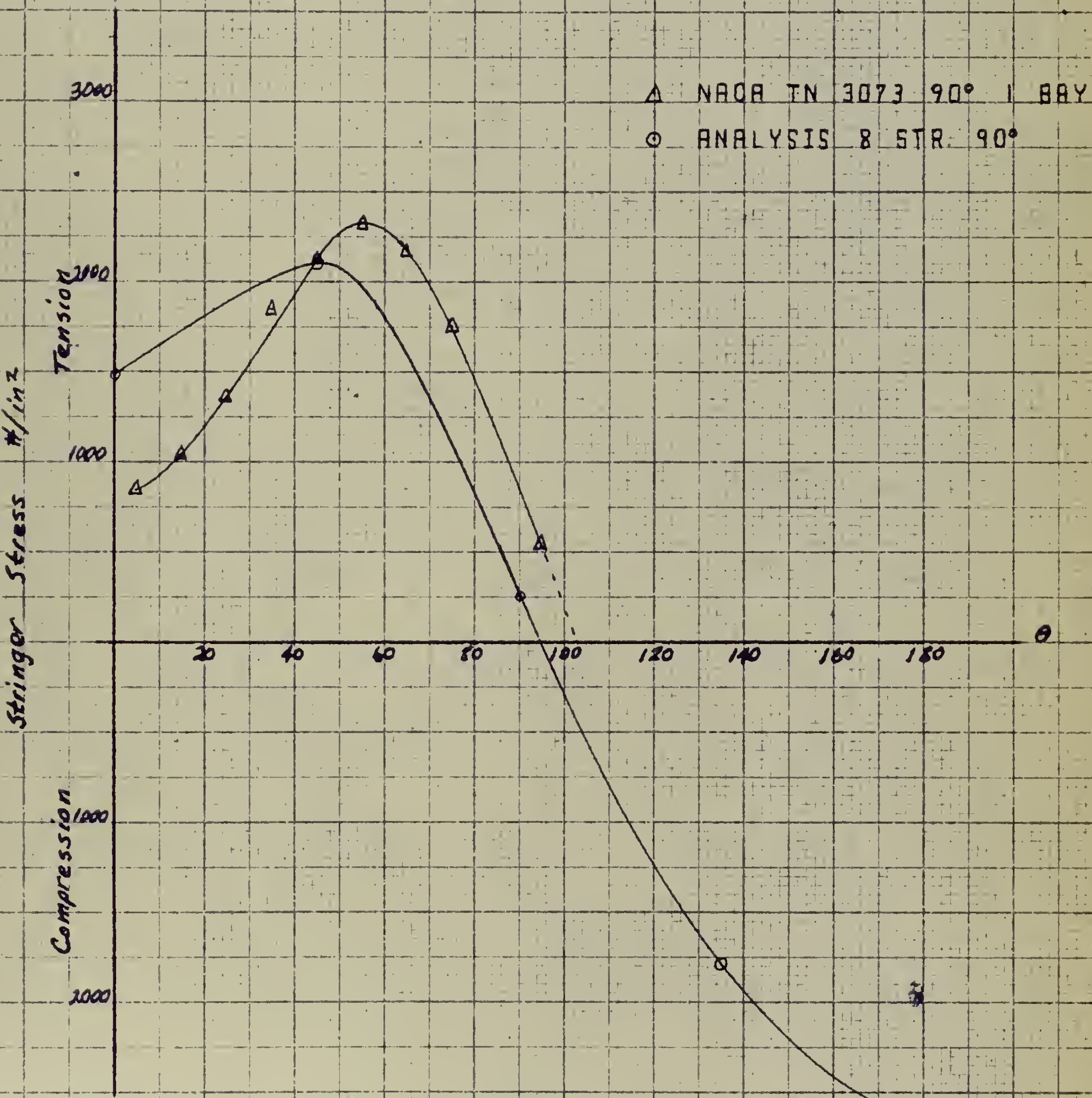

Figure AII - 8

PANEL SHEAR STRESS

CENTER BAY 1

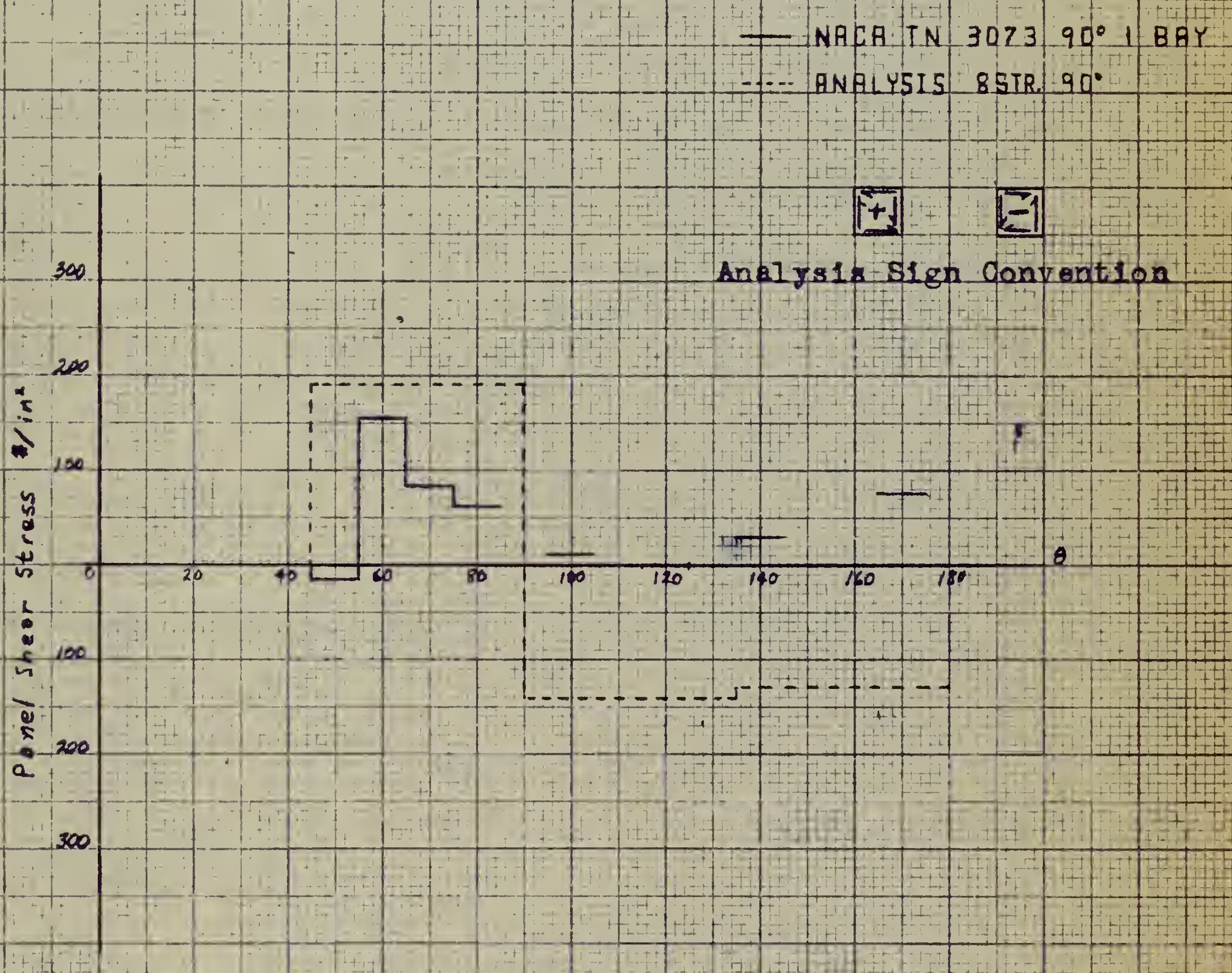

IV. TWELVE STRINGER COMPARISON

In order to achieve a 120 degree cutout, the three patterns must be superimposed with the applied moment to produce zero load in the bottom stringer and in the two lowest side stringers. In addition, the four lowest shear panels must have zero shear. The following four elimination equations result.

1. $q_{s1①}\ell = -q_{s2①}\ell - q_{a1①}\ell - q_{a2①}\ell$
2. $q_{s3①}\ell = q_{s2①}\ell + \frac{1}{2} q_{a2①}\ell$
3. $f_{s3} = f_{s2} + \frac{1}{2} f_{a2} + \frac{\sqrt{3}}{2} F_m$
4. $f_{a1} = -f_{s1} - f_{s2} - f_{a2} - \frac{1}{2}(1+\sqrt{3}) F_m$

Figures AII - 9, 10, and 11 give the comparison plots with reference data for the 130 degree cutout.

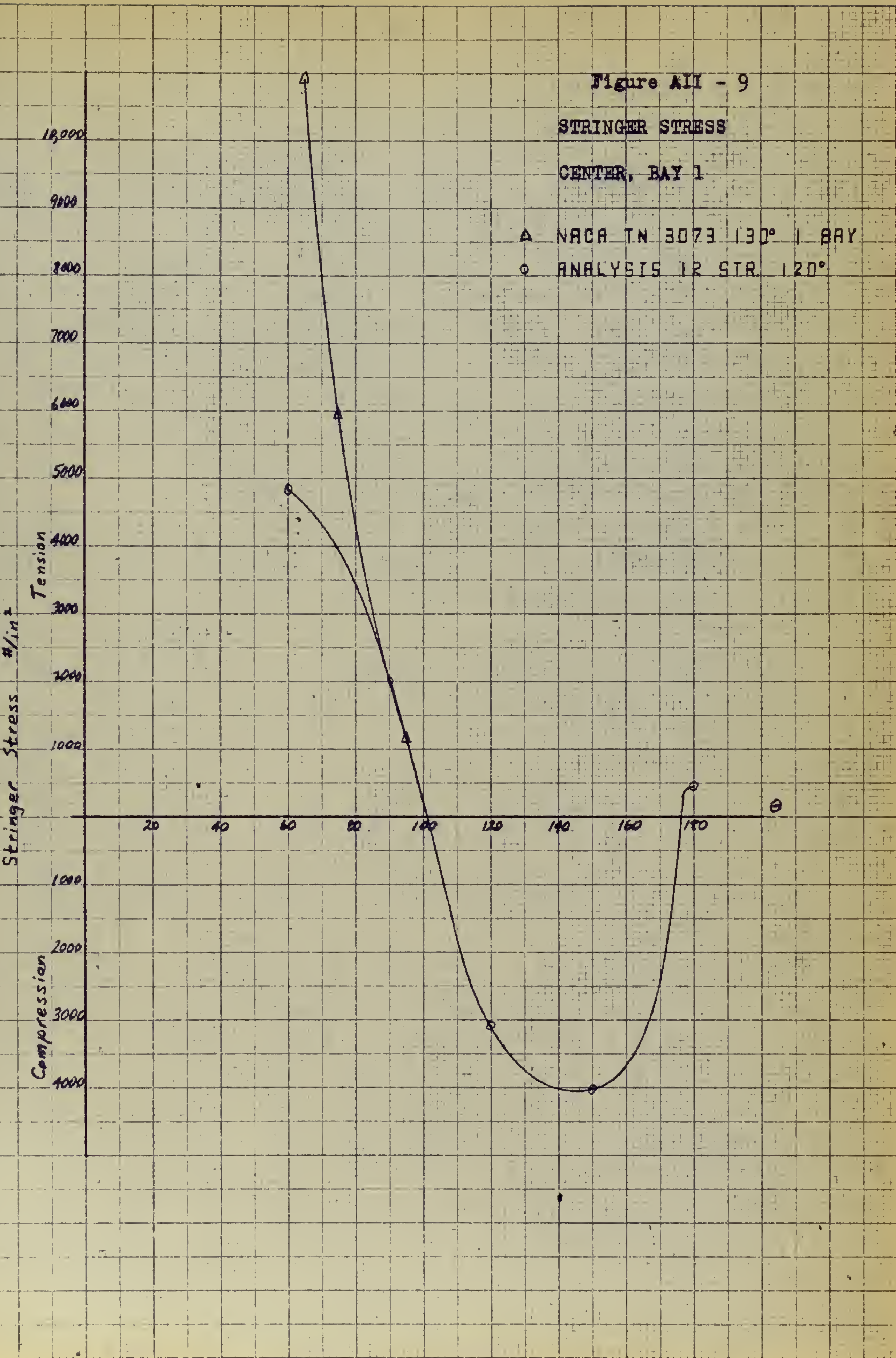
Figure AII - 9
STRINGER STRESS
CENTER, BAY 1
NACA TN 3073 130° 1 BAY
ANALYSIS 12 STR 120°
Stringer Stress #/in²
Tension
Compression
10,000
9000
8000
7000
6000
5000
4000
3000
2000
1000
1000
2000
3000
4000
20
40
60
80
100
120
140
160
180
θ

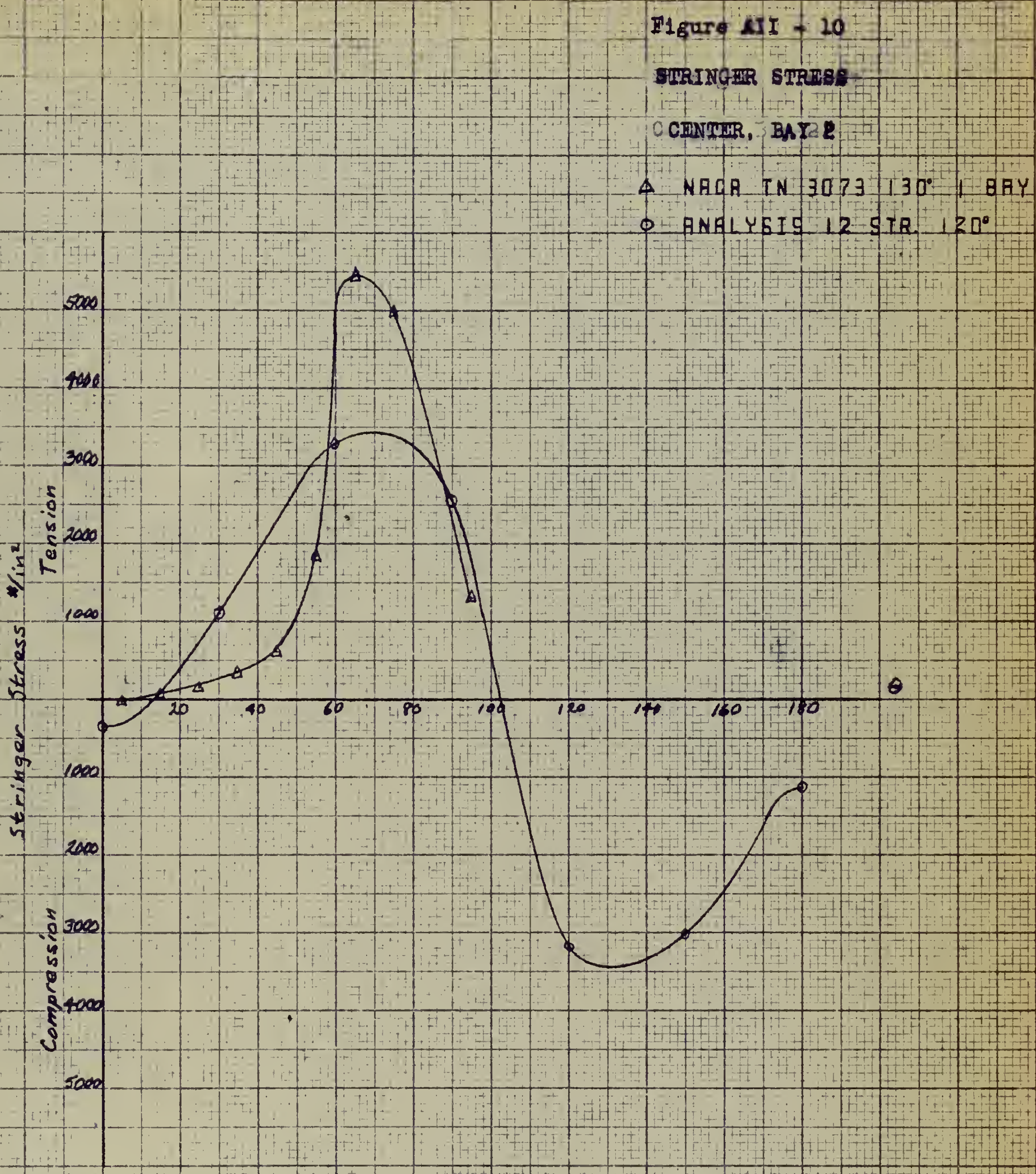
Figure AII - 10
STRINGER STRESS
CENTER, BAY 2
NACA TN 3073 130° 1 BAY
ANALYSIS 12 STR. 120°
Stringer Stress #/in²
Tension
Compression
5000
4000
3000
2000
1000
1000
2000
3000
4000
5000
20
40
60
80
100
120
140
160
180
θ

Figure AII - 11

STRINGER STRESS

CENTER, BAY 3